IAEA-TECDOC-1609

Intercomparison of Techniques for Inspection and Diagnostics of Heavy Water Reactor Pressure Tubes

Determination of Hydrogen Concentration and Blister Characterization

IAEA
International Atomic Energy Agency

March 2009

IAEA-TECDOC-1609

Intercomparison of Techniques for Inspection and Diagnostics of Heavy Water Reactor Pressure Tubes

Determination of Hydrogen Concentration and Blister Characterization

IAEA
International Atomic Energy Agency

March 2009

The originating Section of this publication in the IAEA was:

Nuclear Power Technology Development Section
International Atomic Energy Agency
Wagramer Strasse 5
P.O. Box 100
A-1400 Vienna, Austria

INTERCOMPARISON OF TECHNIQUES FOR INSPECTION AND DIAGNOSTICS OF HEAVY WATER REACTOR PRESSURE TUBES: DETERMINATION OF HYDROGEN CONCENTRATION AND BLISTER CHARACTERIZATION

IAEA, VIENNA, 2009
ISBN 978–92–0–100809–1
ISSN 1011–4289

Printed by the IAEA in Austria
March 2009

FOREWORD

Heavy water reactors (HWRs) comprise significant numbers of today's operating nuclear power plants, and more are under construction. Efficient and accurate inspection and diagnostic techniques for various reactor components and systems, especially pressure tubes, are an important factor in ensuring reliable and safe plant operation.

To foster international collaboration in the efficient and safe use of nuclear power, the IAEA conducted a Coordinated Research Project (CRP) on Intercomparison of Techniques for HWR Pressure Tube Inspection and Diagnostics. This CRP was carried out within the framework of the IAEA's Technical Working Group on Advanced Technologies for HWRs (the TWG-HWR). The TWG-HWR is a group of experts nominated by their governments and designated by the IAEA to provide advice and to support implementation of IAEA's project on advanced technologies for HWRs.

The objective of the CRP was to compare non-destructive inspection and diagnostic techniques, in use and being developed, for structural integrity assessment of HWR pressure tubes. During the first phase of this CRP participants investigated the capability of different techniques to detect and characterize flaws. During the second phase participants collaborated to detect and characterize hydride blisters and to determine the hydrogen concentration in zirconium alloys. The intention was to identify the most effective pressure tube inspection and diagnostic methods and to identify further development needs.

The organizations which participated in phase 2 of this CRP are:

- Comisión Nacional de Energía Atómica (CNEA), Argentina;
- Atomic Energy of Canada Ltd. (AECL), Chalk River Laboratories (CRL), Canada;
- Bhabha Atomic Research Centre (BARC), India;
- Korea Atomic Energy Research Institute (KAERI), Republic of Korea;
- National Institute for Research and Development for Technical Physics (NIRDTP), Romania;
- Nuclear Non-Destructive Testing Research and Services (NNDT), Romania.

IAEA-TECDOC-1499, entitled Intercomparison of Techniques for Inspection and Diagnostics of Heavy Water Reactor Pressure Tubes, Flaw Detection and Characterization, which dealt with the results of the collaboration on flaw detection and characterization (phase 1), was issued in May 2006. This publication reports the results of the collaboration on the characterization of hydride blisters and determination of hydrogen concentration in zirconium alloy HWR pressure tubes (phase 2).

The IAEA appreciates the contributions of P. Nanekar (BARC, India), G. Domizzi, M. Ruch and C. Belinco (CNEA, Argentina) in drafting this IAEA-TECDOC. The IAEA officer responsible for this publication was J.H. Choi of the Division of Nuclear Power.

EDITORIAL NOTE

The use of particular designations of countries or territories does not imply any judgement by the publisher, the IAEA, as to the legal status of such countries or territories, of their authorities and institutions or of the delimitation of their boundaries.

The mention of names of specific companies or products (whether or not indicated as registered) does not imply any intention to infringe proprietary rights, nor should it be construed as an endorsement or recommendation on the part of the IAEA.

CONTENTS

1. INTRODUCTION

1.1. Objective

The heavy water reactor (HWR) pressure tube operates under high-temperature high-pressure aqueous environment. Its integrity is central to the safety of HWR. The pressure tube (PT) material (Zircaloy-2 or Zr-2.5% Nb) undergoes corrosion reaction with heavy water coolant during its service life. This reaction releases hydrogen (deuterium), a part of which gets absorbed in the pressure tube material. The hydrogen in PT material can lead to three specific life limiting issues: (i) Delayed hydride cracking (DHC), (ii) Blister formation and cracking and (iii) Hydride embrittlement. DHC and blister can occur at a much lower hydrogen concentration (less than 100 ppm). Hence, it is not only important to monitor PTs periodically for these two damage mechanisms but also estimate the hydrogen concentration for fitness-for-service assessment.

The International Atomic Energy Agency (IAEA) convened two meetings to provide a forum for technical discussion and exchange of information and experience on HWR pressure tube maintenance and replacement, and to provide recommendations to the IAEA for future cooperative activities in this area. These recommendations were taken into account at the first meeting of the International Working Group on Advanced Technologies for Heavy water reactors (IWG-HWR – now called Technical Working Group on Advanced Technologies for Heavy Water Reactors), held in Vienna in June 1997. At this meeting, the IWG-HWR advised the IAEA to convene a consultants meeting to formulate a Coordinated Research Project (CRP) to address the application of advanced technologies to the safety and reliability of HWRs. The consultants meeting, held in Vienna in July, 1999 formulated the CRP entitled Intercomparison of Techniques for Pressure Tube Inspection and Diagnostics. The CRP was broadly divided in to two phases, phase 1 dealing with 'Flaw characterization by in-situ NDE techniques' and phase 2 dealing with 'Blister characterization by in-situ NDE technique' and 'Determination of hydrogen in zirconium alloy components'. Phase 1 of the CRP concluded in October 2005 and an IAEA-TECDOC-1499 was issued in May 2006 [1]. This IAEA-TECDOC deals with phase 2 of this CRP.

One of the tasks of phase 2 is the determination of hydrogen concentration in PTs. The solubility of hydrogen in zirconium alloys is negligible at room temperature. It increases progressively with temperature and reaches about 60 ppm at 300^{o}C, the operating temperature of PTs. Hydrogen in excess of the Terminal Solid Solubility (TSS) at any given temperature precipitates as zirconium hydride in the matrix (single phase α in case of zircaloy-2 and two phase $\alpha + \beta$ in case of Zr-2.5% Nb). The concern about initiation and growth of DHC puts the limit on maximum amount of hydrogen that can be tolerated in the PT material during its service life. It is therefore important to periodically determine the hydrogen concentration in few PTs. This is done by taking out a scrape sample and then analyzing it by various methods. This is a standard practice, which is being followed in countries operating HWRs. The techniques, instruments, reference standard and analysis procedure, however may differ from one country to another. An intercomparison of these techniques used by different laboratories for hydrogen analysis on scrape samples is therefore of great interest. Such exercise would be useful to add confidence in the measurement techniques and also to establish a few standardized techniques applicable to PTs. Some countries are working towards development of NDE techniques for the determination of hydrogen concentration. Application of NDE methods for hydrogen determination will not only do away with scraping operation but would also allow repeated measurements at the same location over a period of time. However, the sensitivity and the reliability of these techniques need to be demonstrated before their on-site implementation. The objective of this CRP was to compare various destructive methods employed by participating laboratories and also assess the effectiveness of NDE methods for hydrogen measurement in PTs.

The other task of phase 2 of this CRP is blister characterization by in-situ NDE methods. During its service, PT can come in contact with calandria tube (CT) depending on the location of garter spring spacers, creep rates, etc. Zirconium hydride blister may form at the point of contact depending on the hydrogen/deuterium concentration in PT. The blister is brittle, has a larger volume and therefore can crack after reaching a critical size. The presence of cracked blister is a matter of concern from

structural integrity point of view. It is therefore of great importance to be able to detect blister during in-service inspection by NDE methods. It is also of interest to determine whether the blister shows initiation of cracks. The objective of this CRP is to identify reliable NDE methods for blister detection and characterization in PTs.

1.2. Importance of work

Determination of hydrogen concentration in PTs is of great importance to analyse whether: (i) there is a possibility of delayed hydride cracking initiation and growth and (ii) there is a likelihood of blister formation in PTs which are in contact with calandria tubes. The regular practice is to take out the scrape sample and analyze it by various techniques. These techniques differ from one laboratory to other in terms of testing procedure, reference standard, instrument, etc. It is therefore important to compare the various techniques being used by participating laboratories for hydrogen measurement. The CRP allowed the participating laboratories to carry out blind analysis on the samples with varying levels of hydrogen. An accurate estimation of hydrogen would add confidence in the technique(s) employed while inaccurate results would provide information to laboratory whether the existing technique should be improved or replaced by new ones. Some of the laboratories are developing NDE methods for hydrogen determination. The accuracy and sensitivity of NDE measurements needs to be established before they are put to use for in-situ analysis. The CRP also allowed the comparison of the assessment made by NDE with the ones done by more established destructive techniques. This gives very useful information to assess the effectiveness of NDE methods for hydrogen determination and also provide direction for future research in this area.

Detection and characterization of hydride blisters in contacting channels is very important from a safety point of view. Various NDE techniques for blister detection have been developed and standardized in countries operating HWRs. These techniques can be similar to the ones applied for flaw detection or advanced approaches like ultrasonic based velocity ratio measurement, Lamb wave and so on. It is important to demonstrate the reliability of these NDE methods for in-situ blister detection and characterization. The CRP allowed the participating laboratories to try out different NDE techniques on laboratory grown hydride blisters and assess if these are effective to the required level. It also helped in identifying the most suitable NDE technique(s) for this task.

1.3. Scope and process of the CRP

Phase 2 of CRP has two specific tasks: (i) Determination of hydrogen concentration and (ii) Blister detection and characterization by in-situ NDE methods. For hydrogen determination, Zr-2.5% Nb PT samples were charged with varying levels of hydrogen, up to a maximum of 100 ppm. All care was taken to ensure that the hydrogen is uniformly distributed. This was confirmed by metallographic examination. These samples were sent to participating laboratories as per their requirements for hydrogen analysis. Samples were also prepared for non-destructive evaluation and for round-robin analysis. The results from different laboratories were compared with the expected hydrogen concentration in the samples. Comparison was also made between various destructive and non-destructive methods for hydrogen determination.

Blisters were generated in PT samples, which were circulated amongst participating laboratories. The laboratories examined these samples by different NDE techniques. The inspection results from these laboratories were analyzed to ascertain which techniques performed consistently better for blister detection. This analysis helped in identifying reliable NDE technique(s) for in-situ blister detection and characterization.

2. DETERMINATION OF HYDROGEN CONCENTRATION IN ZIRCONIUM ALLOY PRESSURE TUBES

2.1. Contributions from participating laboratories

Table 1 summarizes the methods employed by participating laboratories for hydrogen determination during phase 2 of CRP.

TABLE 1. HYDROGEN ANALYSIS METHODS EMPLOYED DURING CRP

Participating Laboratories	Destructive methods				Non-destructive methods		
	IGF	HVEMS	DSC	DTA	Resistivity	Ultrasonic	Eddy current
CNEA, Argentina	x		x	x		x	x
AECL, Canada		x	x		x		
BARC, India	x	x	x				
KAERI, Republic of Korea	x						
NIRDTP, Romania			x			x	x

2.1.1. Argentina

Argentina prepared 107 samples charged with varying levels of hydrogen for analysis by participating laboratories. Three sets of samples were prepared: (i) analysis by destructive methods by each laboratory, (ii) analysis by non-destructive methods by each laboratory and (iii) samples for round-robin using NDE methods for the intercomparison. Argentina examined the samples prepared by India in addition to its own samples. Argentina employed three techniques for hydrogen analysis: inert gas fusion (IGF), differential scanning calorimetry (DSC) and differential thermal analysis (DTA). Argentina also attempted ultrasonic and eddy current based measurement for determination of hydrogen.

2.1.2. Canada

Canada analysed samples prepared by India and Argentina. Canada employed destructive and non-destructive methods for hydrogen analysis. These analyses were carried out by hot vacuum extraction mass spectrometry (HVE-MS), DSC and resistivity based measurement.

2.1.3. India

India prepared samples charged with varying levels of hydrogen for analysis by participating laboratories. India analysed samples prepared by Argentina in addition to its own samples. India employed three techniques for H analysis: IGF, DSC and hot vacuum extraction quadruple mass spectrometry (HVE-QMS).

2.1.4. Republic of Korea

The Republic of Korea analysed samples prepared by India and Argentina. These analyses were carried out by IGF.

2.1.5. Romania-NIRDTP

Romania analysed samples prepared by Argentina. These analyses were carried out by DSC. Romania-NIRDTP also attempted ultrasonic and eddy current based techniques for hydrogen assessment.

Romania-NNDT

Romania-NNDT attempted ultrasonic based measurements for determination of hydrogen concentration. However, these experiments were not carried out on samples supplied by Argentina and India. A new technique for acousto-elastic characterization of materials, named ultrasonic spectral goniometry (USG), was applied for investigation of PT samples charged with varying levels of hydrogen (see detailed techniques and results from the laboratory report in the attached CD).

2.2. Sample preparation

2.2.1. Argentinean samples

2.2.1.1. Base material

Argentinean samples were prepared from a Zr-2.5% Nb pressure tube (PT) section provided by Canada. The initial hydrogen content in this sample was ~3 ppmw. The PT section was cut into coupons and subjected to the hydrogen charging processes after mechanically removing the oxide layer.

2.2.1.2. Hydrogen charging process

Hydrogen charging was performed in a Sievert device, which consists of a chamber (a quartz tube connected to a high vacuum system consisting of rotary and a turbo molecular pumps) and a hydrogen gas injection system (99.999% purity). The pressure was measured with a cold cathode gauge (10^{-2} to 10^{-8} torr) and a capacitance diaphragm gauge (0.01 to 100 torr). An instrumented furnace with PID controllers was used for heating the samples. Temperature of the samples was measured using a thermocouple located inside the hydrogenation chamber.

The following two processes were employed for hydrogen charging. In process 1, the hydrogen charging temperature was 700°C (higher than the temperature seen by PT during its lifetime). This temperature was limited to 400°C in process 2 to avoid any microstructural changes during charging process. These two processes are described below:

- **Process 1**: The sample was cleaned with trichlorethylene, dried with ethyl alcohol and the initial weight was measured in a microbalance. The sample was loaded in a vacuum chamber and subjected to degassing to remove the initial hydrogen by heating it to temperature of 650-750ºC for 20 min, under dynamic vacuum (10^{-6} to 7×10^{-7} torr). The chamber was removed from the furnace and cooled to room temperature. After isolating the vacuum system, a calculated mass of gaseous hydrogen was introduced into the chamber and the temperature was raised to 700ºC. When the hydrogen absorption was finished, the sample was cooled to room temperature. After this operation, the samples were sealed in a quartz tube and subjected to a homogenization treatment at 500ºC for 103 hours under a high purity Argon atmosphere.

- **Process 2:** The sample was ground with emery paper down to 1200 mesh, cleaned with trichlorethylene, dried with ethyl alcohol and coated with an electro-deposited palladium (Pd)

film. The solution used for the palladium deposition was 0.8g of $PdCl_2$, 0.8g of $NaNO_2$, 2.5g of NaCl, 5 mL of NH_4OH and 100 mL of H_2O. The pH of 11 was obtained by adding 2 drops of HCl. The temperature was held at 40-50°C and the current density was 1.5mA/cm^2. The sample was the cathode and the anode was a palladium coil. The electrolytic deposition was performed for 20 minutes. In order to achieve uniform distribution of hydrogen inside the sample, the palladium film was removed from sample edges (radial-axial and radial-circumferential sections of the PT). This ensured hydrogen ingress in the sample from the major faces only (circumferential-axial surface of the PT). Prior to hydrogen charging, the Sievert device was evacuated to 1 to 5×10^{-6} torr. The hydrogen gas was introduced at room temperature up to a calculated pressure (P_i) and stored in a calibrated chamber (150 mL). The chamber atmosphere was controlled during opening by injecting nitrogen gas to avoid hydriding of the palladium film by the residual hydrogen. One sample at a time was introduced into the hydriding chamber. The chamber was then evacuated with the turbo-molecular pump and heated to 270-290ºC under vacuum (below 1×10^{-5} torr). Finally, the hydriding chamber was isolated from the vacuum system and the stored hydrogen gas was released. After the hydrogen absorption was achieved (less than 10 min), the chamber was removed from the furnace and the final pressure P_f was measured at room temperature. The palladium film was removed by exposure at room temperature to hydrogen gas at 1000 torr. The palladium layer gets hydrided and partially detached from the surface sample. The hydrogen charged samples were homogenized in batches of five samples in a sealed Pyrex tube filled with high purity Argon. The tubes were held at 340 ± 5º C for 240 hours, after which they were removed from the furnace and air-cooled. Samples with 80 ppmw or higher hydrogen concentration were subjected to a second 240 hours of homogenisation heat treatment at 380ºC.

In both processes, the hydrogen concentration (atomic fraction) in each sample was calculated from the difference between the initial and final hydrogen pressures (<0.01 torr) measured at room temperature. This was also confirmed from the initial and the final weight of the sample found out by high precision micro-balance. Detailed information about the above processes can be found in the Argentina report (attached CD).

Sample charged with process 1 were used for analysis by direct methods such as IGF and HVE-MS, while the ones charged with process 2 were used for analysis by indirect methods such as DSC, DTA and NDE. Process 2 samples were also analysed by HVE-MS (Canada) to confirm the correctness of the expected hydrogen concentration.

2.2.1.3. Sample cutting and identification

The specimens for IGF, HVEMS, DSC and DTA were cut with a diamond wheel-sectioning machine according to size requirements of each laboratory. The specimens for NDT measurements were labelled and distributed to each laboratory. Details can be found in Argentinean report (attached CD).

2.2.1.4. Microstructure

Figure 1 shows microstructure of the pressure tube in as-received condition. This tube was provided by AECL, Canada. Figure 2 and Figure 3 show the distribution of hydride platelets in samples hydrided by process 1 and process 2, respectively. The hydride platelets in samples produced by process 1 show some branches in both, circumferential and radial directions. On the other hand, the hydride platelets obtained with process 2 are parallel to the circumferential-axial plane of the PT, which is similar to the one observed in as-fabricated Zr-2.5%Nb PT.

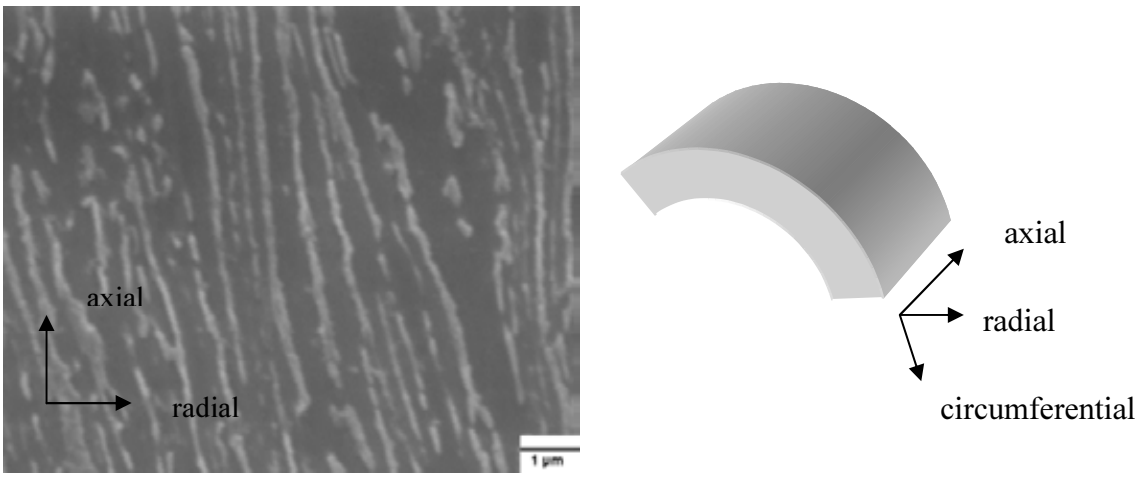

FIG. 1. Microstructure of the Canadian PT (as received, axial-radial plane).

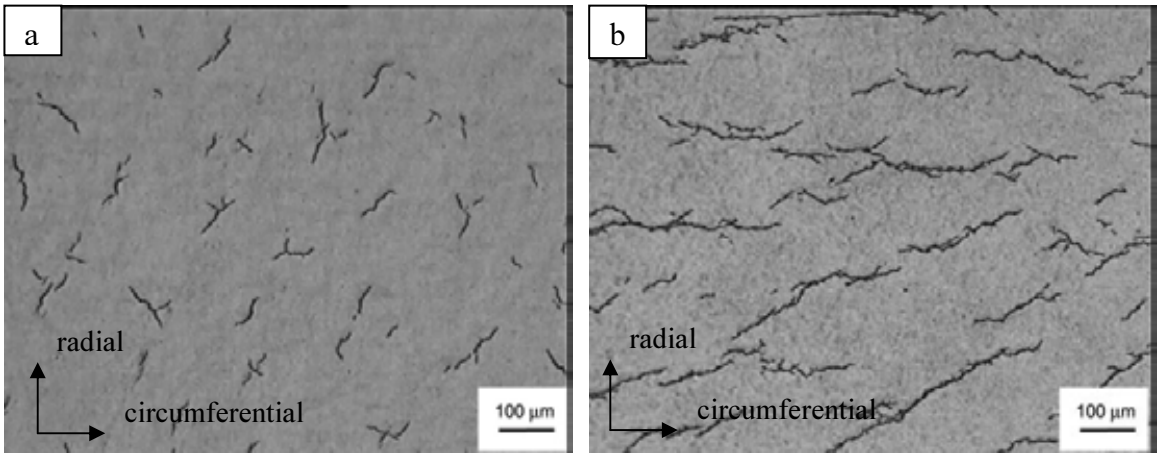

FIG. 2. Samples prepared with process 1 Argentina, a) 25 ppmw H and b) 83 ppmw H.

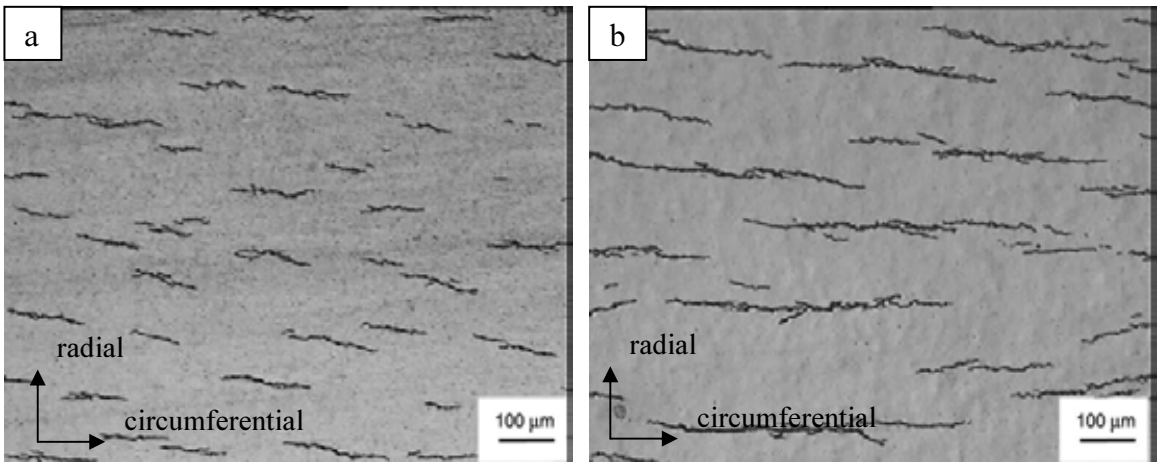

FIG. 3. Samples prepared with process 2 Argentina, a) 24 ppmw H and b) 77 ppmw H.

2.2.2. Indian samples

2.2.2.1. Base material

The base material for the Indian samples was a PT section belonging to India. The initial hydrogen content in the PT section was approximately 5 ppmw. The PT fabrication route involves a two-stage pilgering (Cold Work) with an intermediate heat treatment at 550 ºC. After the final pilgering, the PT is stress relieved in an autoclave at about 400 ºC for 24 hours.

2.2.2.2. Hydrogen charging process

The hydrogen charging set-up consists of a main glass manifold connected with calibrated volumes, uranium (U) traps charged with hydrogen, two gas independent capacitance diaphragm gauges in which one reads pressure in the range of 1 to 10^{-4} mbar and the other in the range of 0.01 to 100 mbar and a quartz heating tube, 32 mm ID, with a ground glass joint and an O ring seal. The U traps and the sample charging furnaces were provided with K-type thermocouples and programmable PID controllers, which control the furnace temperatures within ±1ºC. The system was connected to a turbo molecular pumping system along with a liquid nitrogen trap, which can achieve a vacuum of approximately 10^{-7} mbar in a short time. The system leak rate was less than 1.5×10^{-7} mbar l/s. A schematic view of the Hot Vacuum Extraction-hydrogen charging system and its details are given in the India report (attached CD).

During charging, importance was given to generate samples with uniform and precisely known amounts of hydrogen. The microstructural changes during the charging process were not considered a matter of concern. The PT samples were ground to remove the oxide layer and their surfaces were cleaned in a non-hydrogenous solvent (CCl_4) in an ultrasonic cleaner. A known amount of hydrogen gas was collected in a separate volume. The cleaned and dried Zr alloy sample was weighed using a microbalance and loaded into the Hot Vacuum Extraction (HVE) charging system. The sample was first held at about 200°C for 10 min in a vacuum to drive out the adhering volatile components on the sample surface (degassing) and then subjected to de-charging at 1030°C for 60 min in a vacuum of $\sim 10^{-6}$ mbar. The system was isolated and a calculated quantity of hydrogen gas was brought in contact with the sample. The maximum amount of hydrogen was absorbed between 750°C to 800°C. The samples were then subjected to homogenisation at 750°C for 28 hours followed by slow cooling to ambient temperature at the rate of 1°C/min to ensure uniform distribution of hydride platelets. The complete hydrogen charging heat treatment cycle is presented in the India report (attached CD).

Ten sets of Zr–2.5% Nb alloy coupons were charged using high purity hydrogen gas to the concentration levels of 20, 40, 60, 80 and 100 ppmw within an accuracy of ± 2 ppmw. The extent of de-charging of initial hydrogen was only marginal (less than 3 ppmw) for the biggest coupons of size 20 × 20 × 4 mm. Hence, the hydrogen concentration was calculated from the difference between the initial and final pressure of the hydrogen gas and the initial hydrogen concentration. The difference in weight of the sample after and before charging was also used to estimate the expected hydrogen content in the samples. Two sets of samples (three coupons per set) of equivalent surface area to weight ratio could be charged successfully to the same hydrogen concentration level in a single charging run.

2.2.2.3. Sample identification

The coupons were subsequently sliced according to the requirements of the different laboratories. Samples from the first set of charging were dispatched to Argentina (three slices from each concentration) and Republic of Korea (five slices from each concentration). One sample from each coupon was kept in India as a reference. Samples from the second set were sent to Canada (three slices from each concentration) and to Romania (one coupon of size 20 × 20 × 4 mm from each concentration). The Samples were labelled ARG -1 to ARG- 6, KOR -1 to KOR- 6, CAN-1 to CAN-6

and ROM-1 to ROM-6. Refer to the India report on the attached CD for all sample weights and their identification labels.

2.2.2.4. Microstructure

Figure 4 shows the microstructure of two samples charged by India. Since the charging was carried out at high temperature the alloys transforms into β phase and re-transforms during cooling into Widmanstatten structure. Indian samples present thicker and fewer hydride platelets than Argentinean ones.

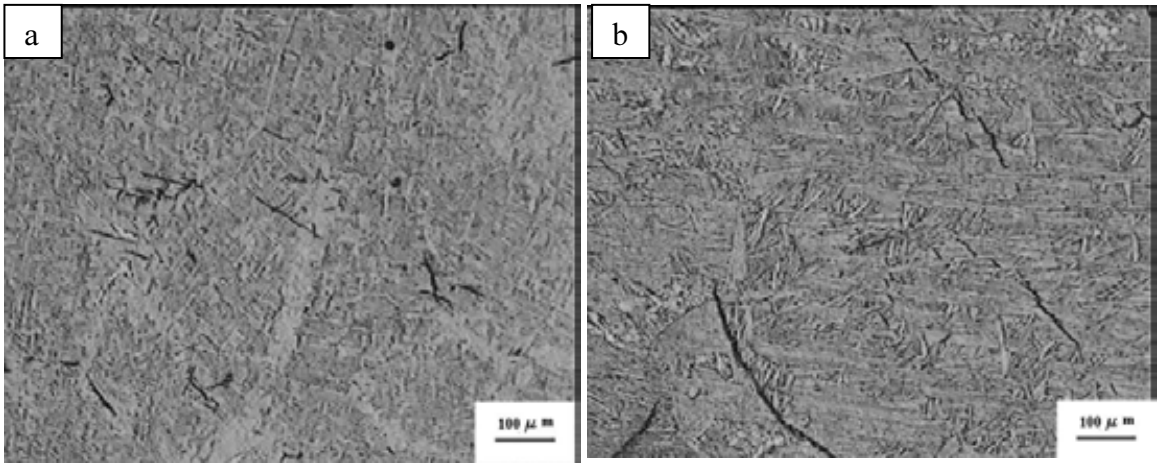

FIG. 4. Samples prepared by India, a) 20 ppmw H and b) 80 ppmw H.

2.3. Hydrogen determination techniques for pressure tubes

The techniques used during this phase of CRP for hydrogen determination are broadly classified into two categories: Destructive and Non-Destructive. In Destructive Tests, a distinction is made between direct methods and indirect methods. All methods using NDE are indirect methods.

Direct methods involve taking a scrape sample from PT. In direct methods (HVE-MS and IGF), the total amount of hydrogen in the sample is measured directly. However, the specimen can be used only once as hydrogen contained in the sample is driven out and the sample is destroyed during the analysis. In indirect methods, (DSC and DTA) hydrogen measurement is based on determination of a precipitation or dissolution temperature of hydrides in zirconium matrix. The hydrogen concentration is then assessed indirectly from this temperature and the solvus curve. In these tests, the sample is not destroyed and as a result several measurements can be made on a single sample. However, these methods cannot be applied in-situ and the analysis needs a small PT sample, which is again drawn by scraping.

NDE methods for hydrogen determination are based on change in some parameter (sound velocity, attenuation, conductivity, etc.) due to presence of hydride in zirconium matrix. These measurements can either be static or dynamic (heating or cooling cycle). NDE methods have the potential for in-situ hydrogen assessment in PTs. The advantage of NDE method(s) is that it does not need scraping of a PT. As a result any possible damage of a PT during scraping operation is avoided. Secondly, one can take repeated measurements at the same location over a period of time to assess the hydrogen pick-up rate. The amount of hydrogen required to be sensed by NDE method is of the order of 100 ppm or less. Such a small amount of hydrogen does not cause an appreciable change in NDE parameters. Moreover, there are other effects like microstructural changes due to long-term high temperature exposure, radiation damage, texture variation, etc. whose effects on NDE parameters need to be accounted for. These are some of the difficulties, which make development and application of an NDE method for hydrogen determination in PT a challenging task. During this CRP, the participating

laboratories attempted ultrasonic, eddy current and resistivity based measurement for determination of hydrogen.

The details regarding the type of instrument and the calibration standard used by participating laboratories using direct methods (HVE-MS and IGF) are given in Table 2. The experimental details for dynamic methods (DSC, DTA and Resistivity) are given in Table 3. More information on the process details can be found in the reports from participating laboratories (attached CD).

TABLE 2. EXPERIMENTAL DETAILS FOR HVE-MS AND IGF ANALYSIS

Country	Method	Equipment	Hydrogen Standard or Reference Material	Weight of Standard (mg)	Nominal C_H (ppm)	Measured C_H (ppm)
Argentina Lab1	IGF	LECO RH-404	LECO: 501-529 762-741,502-154 Arg. samples	-	5.9 ± 0.5 32 ± 3.2 80.4 ± 5.8	5.9 32 80.4
Argentina Lab 2	IGF	LECO RH-404	Titanium Arg. samples	-	20.6±1.2	21.1
Canada	HVEMS	Customized	AECL standard W-33-11	100	9.3	9.5±2.0
			AECL standard 100HA	200	99	97±3
India	IGF	CIC H2002	NBS	101.2	25 ± 4	21.4
			NBS	101.9	25 ± 4	21.4
			Ti	100.8	25	21.8
			Zr-based alloy	100	11±1	10.70
						10.80
	HVE-QMS		Zr-based alloy	100	11±1	9.89
						11.28
						11.55
Republic of Korea	IGF-TCD	LECO RH-404 EF-400	AECL 20HA/100HA (H in Zr-2.5Nb)	-	system blank 0.05 µg/g	

NBS: National Bureau of Standards.

TABLE 3. EXPERIMENTAL DETAILS FOR THE DYNAMIC METHODS (DSC, DTA, RESISTIVITY)

Country	Number of cycles	Heating rate [ºC/min]	Maximum temperature [ºC]	Hold time [min]	Cooling rate [ºC/min]	Purge gas	Gas flow rate [l/h]
Argentina-1 – DSC	3	20	395	5	20	N 99.99%	1.5
Argentina-3 – DSC	3	10	360	0	10	Ar 99.99%	1.8
Argentina-3 – DSC	3	10	400	0	10	Ar 99.99%	1.8
Argentina-4– DTA	3	10	380	0	10	Ar 99.99%	1.5
Canada DSC	3	10	350-380	0	10	N 99.999%	3.0
Canada Resistivity	3	3-5	350-380	0	3-5	Not applicable	Not applicable
India DSC	3	10	400	5	Not applicable	Ar 99.999%	2.4
Romania DSC	3	10	400	5	10	N	11.5

2.3.1. Argentina

Argentina employed IGF, DSC and DTA for hydrogen analysis. Argentina also attempted ultrasonic and eddy current based measurements.

Ultrasonic measurements were made in pulse-echo configuration using 15 MHz, 6.25 mm diameter and 3.75 mm focal length transducer. Signals were acquired at a sampling rate of 100 M samples/sec. These signals were processed with dedicated software, and the velocity was obtained by the cross-correlation method (relative error of $\Delta v/v \approx 0.002$).

For eddy current based measurement, special coils matching tube curvature were prepared. The eddy current tests were performed with a bridge-type equipment. A set of electrical conductivity standards were used for the calibration. The specimens were analysed at frequencies in the range 130 kHz to 820 kHz.

2.3.2. Canada

Canada employed HVE-MS and DSC for hydrogen analysis. Canada also used an NDE technique based on resistivity measurement for assessment of hydrogen concentration.

For resistivity-based measurements, Canada used the bench-top system to determine temperature corresponding to terminal solid solubility for dissolution (T_D) and precipitation (T_P) by measuring sample resistance as a function of temperature. Four-point contact electrical measurements were made to avoid the complications and uncertainties associated with an eddy current system. To do this, holes for connecting the cables were made on the samples supplied by Argentina for non-destructive evaluation (ND samples). The Arrhenius curves from McMinn [2] were used to calculate hydrogen concentration (C_H) from the experimental dissolution and precipitation temperatures (T_D and T_P are respectively the temperature of steepest slope on heating and cooling respectively)

$$C_{du} = 106446.7 \cdot \exp\left(-4328.67 / T_D \right)$$

$$C_{pu} = 138746.0 \cdot \exp\left(-4145.72 / T_P \right)$$

where: C is the hydrogen concentration, in ppmw,

du signifies *d*issolution *u*nirradiated,

pu signifies *p*recipitation *u*nirradiated,

T_D and T_P are changed in equation in order to be consistent with Tables 8 and 9 (K)

2.3.3. India

India employed HVE-QMS, IGF and DSC for hydrogen analysis. A detailed account of these techniques and the analysis procedure can be found in Indian report (attached CD).

2.3.4. Republic of Korea

The Republic of Korea employed IGF for hydrogen analysis. A detailed account of these measurements and the analysis procedure can be found in Republic of Korea report (attached CD).

2.3.5. Romania-NIRDTP

Romania-NIRDTP employed DSC, ultrasonics and eddy current based measurement for hydrogen analysis.

Ultrasonic velocity measurement was carried out using a 10 MHz focused transducer.

Eddy current technique was based on measurement of conductivity using bridge type eddy current equipment. The measurements were made at 40 kHz in the external reference mode. Neural network inversion techniques were applied for data analysis.

2.4. Intercomparison of results

In this section, intercomparison is made between the results obtained by participating laboratories as well between different hydrogen analysis methods. More detailed information on the results from individual laboratories can be found in the laboratory reports (attached CD).

2.4.1. Direct methods (HVE-MS and IGF)

Hydrogen concentration determined by Canada and India using HVE-MS on Indian sample are given in Table 4. Hydrogen concentration determined by Argentina (Lab 1 and Lab 2), India and Republic of Korea using IGF on Indian samples are given in Table 5. The expected hydrogen concentrations in these samples (calculated during the charging process) are reported alongside for the sake of comparison.

TABLE 4. HVE-MS RESULTS ON SAMPLES PREPARED BY INDIA

Expected Concentration (ppmw)	Measured Concentration (ppmw)	
	Canada	India
≤5	2.1	Not measured
20	23	24.4
40	42	Not measured
60	62	64.5
80	79	83.6
100	99	Not measured

TABLE 5. IGF RESULTS ON SAMPLES PREPARED BY INDIA

Expected Concentration (ppmw)	Measured Concentration (pppmw)					
	Argentina				Republic of Korea	India
	Lab 1		Lab 2			
≤ 5	3.5	3*	1	12*	3.2	-
20	24	25 *	4	27*	26.2	22.4
40	58	46*	6	35*	46.2	39.6
60	83	72*	12	60*	68.9	61.9
80	105	87*	14	72*	87.5	79.4
100	129	115*	19	74*	109.6	98.7

* Measured after checking calibration with an Argentinean sample charged with process 1.

The results of direct methods on samples prepared by Argentina by process 1 and by process 2 are given in Table 6 and Table 7 respectively. From each coupon, identified by a particular hydriding label, several specimens were cut and distributed amongst the laboratories. Results from a particular coupon are displayed in the same row (or group of rows).

The information in Tables 4 to 7 is plotted in Figures 5 and Figure 6. Information on sample labeling, sample mass, expected and measured concentration, etc. is given in Argentina and India reports (attached CD).

TABLE 6. RESULTS ON SAMPLES PREPARED BY ARGENTINA (PROCESS 1)

Hydriding Label	Expected Concentration (ppmw)	Measured Concentration (ppmw)					
		IGF				HVEMS	
		Argentina		Rep. of Korea	India	Canada	India
		Lab 1	Lab 2				
0	3	2.9 | 3.0 *	1.7	32.2	2.1	1.8±0.8	5.8
			1.3	3.5	2.8		4.3
			2.1	4.1	1.7		4.9
10	25.0±1.0	-	3.7	31.3	28.4	27 ± 1	24.35
							45.54
							49.11
6	25.2±1.0	-		34.9	25.0		
					25.2		
1	54.5±1.7	-	7.7	70.8			41.96
		-					49.39
							39.15
							52.00
2	57.6± 1.9		53 49.3 77.9*				
5	56.8±1.8		8.4	65.4	50.8	56 ± 3	
					53.7		
3	55.3	-		68.5	53.8		
					49.1		
9	64.9±2.2	86 - 93 | 78 *		77.0	59.6	63 ± 3	74.84
							74.56
							53.82
4	63.8±2.1			74.6	60.1		
				63.8	58.6		
7	82.6±3.1	-	18.5	98.7	75.6	77 ± 4	68.65
							67.70
							72.20
8	82.2±3.0		15.3	95.4	75.1		
					74.7		

* Measured after checking calibration with an Argentinean sample charged with process 1.

TABLE 7. RESULTS ON SAMPLES PREPARED BY ARGENTINA (PROCESS 2)

Hydriding Label	Expected hydrogen Concentration (ppmw)	Measured Concentration (ppmw)				
		IGF				HVEMS
		Argentina			Republic of Korea	Canada
		Lab 1		Lab 2		
P-1-1	26.6 ± 3			6.4	47.0	
P-1-2	26.6 ± 3	39.5	42 *	6.4		40 ± 2
						39 ± 2
P-2-1	53.8± 3.6			10.6		71 ± 4
						68 ± 4
P-2-2	56.8± 3.7	79 83	73 *			
				9.0		
P-3-1	80.5±4.8			14.2	107.0	94 ± 5
P-3-2	79.7± 4.7	102 112	96 *			87 ± 5
ND-0-2	3 ± 1					3 ± 1
ND-1-2	26.3 ± 3					48 ± 3
ND-2-2	53.4 ± 3.5					77 ± 4
ND-3-2	80.3 ± 5.8					95 ± 5
ND-0-1	3 ± 1					13 ± 2
ND-1-1	26.7± 3					49 ± 3
ND-2-1	52 ± 3.5					77 ± 4
ND-3-1	82.5 ± 5.8					84 ± 4

* Measured after checking calibration with an Argentinean sample charged with process 1.

The hydrogen concentrations reported by Canada using HVE-MS on the samples charged by Argentina with process 2 are higher than expected (calculated from the gaseous charge plus the 3 ppmw original concentration). During the deposition of palladium film, protons of the electrolytic solution collide with the sample. Then it is likely that an additional pick up of hydrogen might have taken place during the palladium deposition, which was not accounted for while arriving at the expected hydrogen concentration. In order to confirm this, a sample was covered with palladium and then exposed to a 30 minutes heat treatment at 290ºC, similar to that received by the samples charged with process 2, but under higher vacuum. Hydride precipitation near the surface was observed by metallography (Figure 7). This study shows that process 2 is not an appropriate method to produce standards with a known hydrogen concentration, at least in the lower range (3-80 ppmw). For these samples a correction for hydrogen pickup must be made before they are used in such exercise. Process 2 samples were utilized during this CRP for measurements using DSC, DTA and NDE. In view of the above, the hydrogen concentration determined by Canada using HVE-MS is considered as the expected hydrogen concentration in these samples.

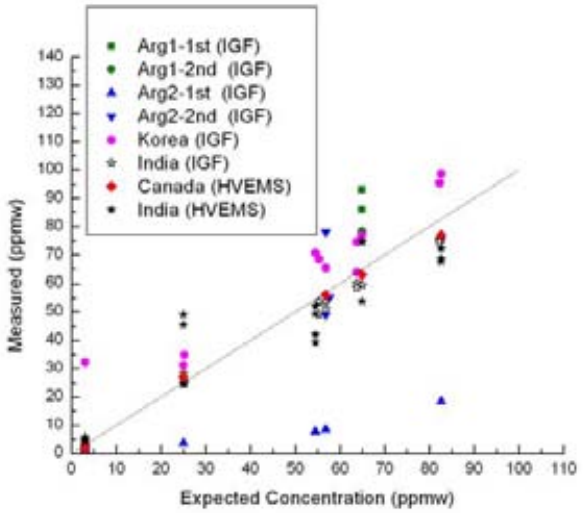

FIG. 5. Results of IGF and HVEQMS measurements on samples prepared by Argentina, process 1.

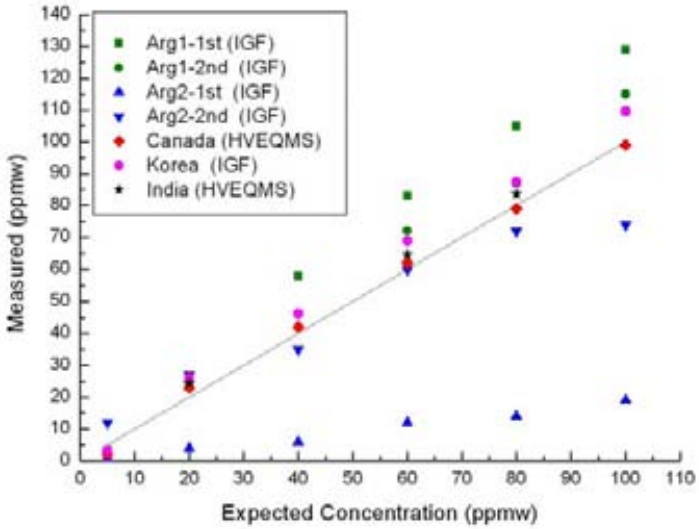

FIG. 6. Results of IGF and HVEQMS measurements on samples prepared by India.

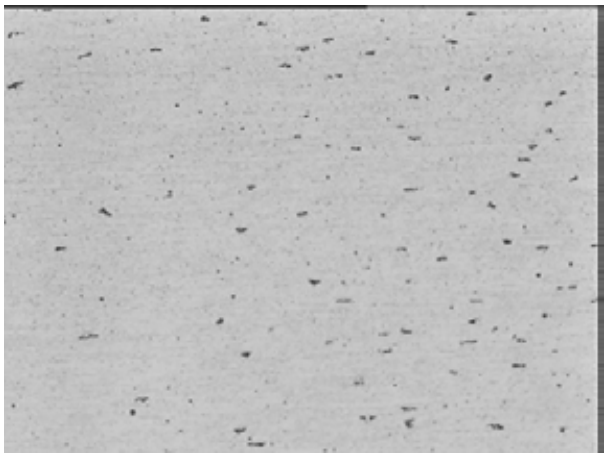

FIG. 7. Hydride particles in the sample covered with palladium and heat treated at 290°C for 30 min under high vacuum after removal of the palladium film.

2.4.2. Indirect methods (DSC, DTA, resistivity, ultrasonics and eddy currents)

The hydride dissolution and precipitation temperatures measured by the different laboratories are reported using the definitions in the calorimetric curves by Mc Minn as shown in Figures 8a and 8b:

- T_{mD} = temperature of the minimum of the calorimetric curve on heating or dissolution or peak temperature;
- T_{mP} = temperature of the maximum of the calorimetric curve on cooling or precipitation or peak temperature.
- T_{SSH} = temperature of the steepest slope on heating or maximum slope temperature;
- T_{SSC} = temperature of the steepest slope on cooling or maximum slope temperature;
- T_{onset} = temperature of the precipitation or dissolution beginning.

All the participating laboratories agreed to discard the first run during analysis by DSC. This is due to the fact that the first run contains signals corresponding to various irreversible changes such as relaxation of residual stresses and other effects caused by sampling processes. The average of the second and third runs is presented in Table 8 and Table 9 for heating and cooling respectively. Detailed Information (Sample label, hydriding label, expected concentration, sample mass, enthalpy change and the different temperature values measured in each run) is reported in the attached CD.

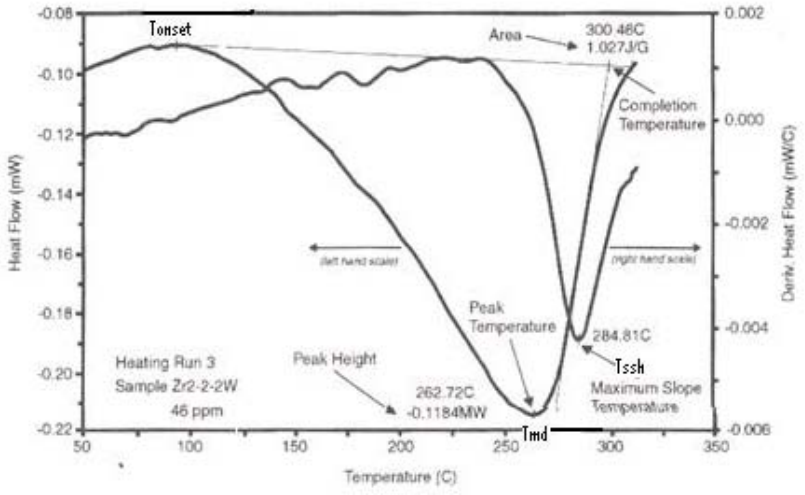

FIG. 8a. Calorimetric curves for Zr-H, showing temperature definition for heating [2].

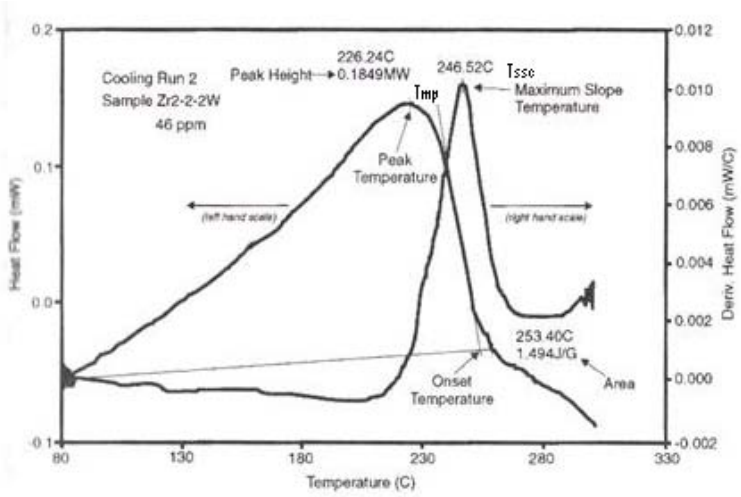

FIG. 8b. Calorimetric curves for Zr-H, showing temperature definition for cooling [2].

TABLE 8A. DSC RESULTS ON ARGENTINEAN SAMPLES (PROCESS 2) DURING HEATING (AVERAGE OF 2nd AND 3rd CYCLE)

Hydriding label	Measured by Canada using HVE-MS (ppmw)	T_{mD}					T_{SSH}				
		395	400	400	360	360	395	400	400	360	360
		DSC Arg Lab 1	DSC Arg Lab 3	DSC India	DSC Arg Lab 3	DSC Can	DSC Arg Lab 1	DSC Arg Lab 3	DSC India	DSC Arg Lab 3	DSC Can
a	3#	ND	-	169.2	-	ND	ND	-	173.2	-	ND
b	3#	ND	-	150.9	-	ND	ND	-	156.4	-	ND
c	3#	-	-	150.5	-	ND	-	-	155.9	-	ND
p-1-1	39-40**	271	253.5	268.8	256.5	-	278	281.5	281.0	286	-
		271	-	269.5*	-	-	279	-	282.3*	-	-
p-1-2	39-40	268	254.5	264.3	260	259.3	274	273	276.0	269.5	277.3
		-	-	-	-	260.3	-	-	-	-	277.4
		-	-	-	-	260.3	-	-	-	-	277.3
p-2-1	71-68	306	-	299.3	-	301.5	316	-	319.0	-	319.4
		307	-	-	-	298.0	315	-	-	-	316.3
p-2-2	71-68**	304	266	303.5	268	299.1	312	321.5	317.1	317.5	316.7
		-	-	304.0*	-	-	-	-	317.5*	-	-
p-3.-1	94	330	-	329.3	-	324	340	-	347.1	-	345.1
		332	-	-	-	-	341			-	-
p-3-2	87	328	321*	324.8	320	320.1	339	342*	340.5	341	338.2
		-	-	324.0	-	319.9			342.1		339.6

ND: non detected.
Not measured by HVE-MS. Initial hydrogen concentration in as-received pressure tube sample.
* 2nd run only.
** Not measured by HVE-MS. The concentration of p-1-1 was assumed to similar as for p-1-2, and p-2-2 was assumed to be similar as for p-2-1, since the targeted concentration in the respective samples were identical in these two cases.
+ DTA measurements were not performed during heating and hence no data is reported in this table.

TABLE 8B. DSC AND RESISTIVITY RESULTS ON ARGENTINEAN SAMPLES (NDE SAMPLES) DURING HEATING (AVERAGE OF 2nd AND 3rd CYCLE)

Hydriding Label	Measured by Canada using HVE-MS (ppmw)	T_{mD}		T_D	T_{SSH}	
		400	360	Resistivity	400	360
		DSC Rom	DSC Can	Can	DSC Rom	DSC Can
ND 1-2	48	-	278.3	288		292.1
ND 2-2	77	-	310.2	320		326.4
ND 3-2	95	-	326.8	340		346.2
ND 0-1	13	-	173.7	-		197.4
ND 1-1	49	-	271.7	277		287.5
ND 2-1	77	-	305.4	312		322.4
ND 3-1	84	-	314.2	328		332.6
ND 0-4	-	ND	-	-	Not reported	-
ND 1-4	-	315	-	-	Not reported	-
ND 2-4	-	293	-	-	Not reported	-
ND 3-4	-	310	-	-	Not reported	-

TABLE 9A. DSC RESULTS ON ARGENTINEAN SAMPLES (PROCESS 2) DURING COOLING (AVERAGE OF 2ND AND 3RD CYCLE)

Hydriding label	Measured by Canada using HVE-MS (ppmw)	T_{mP}					T_{SSC}					T_{onset}
		395	400	400	360	380	395	400	400	360	360	360
		DSC Arg Lab 1	DSC Arg Lab 3	DSC India#	DSC Arg Lab 3	DTA Arg Lab 4	DSC Arg Lab 1#	DSC Arg Lab 3	DSC India#	DSC Arg Lab 3	DSC Can	DSC Can
a		ND	-	-	-	-	-	-	-	-	ND	ND
b		ND	-	-	-	-	-	-	-	-	ND	ND
c		ND	-	-	-	-	-	-	-	-	ND	ND
p-1-1	39-40**	197	217	-	223	243	-	222	-	228.5	-	-
		198	-	-	-	-	-	-	-	-	-	-
p-1-2	39-40	191	210	-	218	-	-	215.5	-	224	223.7	231.0
		-	-	-	-	-	-	-	-	-	216.8	222.7
		-	-	-	-	-	-	-	-	-	217.0	224.3
p-2-1	71-68	243	-	-	-	255	-	-	-	-	269.5	276.1
		242		-	-	-	-	-	-	-	265.4	270.5
p-2-2	71-68**	238	259.5	-	262	-	-	262.5	-	273.5	269.2	275.8
p-3.-1	94	277	-	-	-	265	-	-	-	291	295.0	301.3
		275	-	-	-	-	-	-	-	-	-	-
p-3-2	87	269	283	-	281	-	-	288.5	-	289	289.4	297.7
		-	-	-	-	-	-	-	-	-	289.1	295.4

** Not measured by HVE-MS. The concentration of p-1-1 was assumed to similar as for p-1-2, and p-2-2 was assumed to be similar as for p-2-1, since the targeted concentration in the respective samples were identical in these two cases.

Data not acquired during cooling.

TABLE 9B. DSC AND RESISTIVITY RESULTS ON ARGENTINEAN SAMPLES (NDE SAMPLES) DURING COOLING (AVERAGE OF 2ND AND 3RD CYCLE)

Hydriding label	Measured by Canada using HVE-MS (ppmw)	T_{mP}	T_P	T_{SSC}		T_{onset}
		400		400	360	360
		DSC Rom	Resistivity Can	DSC Rom	DSC Can	DSC Can
ND 1-2	48		241		234.0	240.4
ND 2-2	77		282		275.7	281.5
ND 3-2	95		302		295.4	303.4
ND 0-1	13		182		191.5	198.5
ND 1-1	49		228		228.8	237.0
ND 2-1	77		263		271.1	278.1
ND 3-1	84		284		281.0	288.0
ND 0-4	-	-	-	-	-	-
ND 1-4	-	-	-	-	-	-
ND 2-4	-	-	-	-	-	-
ND 3-4	-	-	-	-	-	-

Results of resistivity-based measurements from Canada are presented in Table 8 and Table 9. Linear and quadratic least-squares curve fits were made to the resistance vs. temperature relationship. The residuals from these curve fits were then plotted and the T_D and T_P (dissolution and precipitation) temperatures were estimated as illustrated in Fig. 9. T_P was selected as the temperature at the (local) peak in the residual for the cool-down. Selection of T_D is not as clear-cut. The expression given in the C_H vs T Arrhenius curve is based on complete hydride dissolution. Hence, the point indicated in Figure 9 was used for T_D, under the assumption that when the residual became fairly linear, the dissolution was complete.

Figure 10 to Figure 13 show the plots of T_{mD}, $T_{SSH,}$ $T_{SSC,}$ T_{mP} and T_{onset} measured values obtained by DSC and DTA methods, respectively, against the hydrogen concentration determined by Canada using HVE-MS. Several terminal solid solubility curves for dissolution and precipitation (TSS_D and TSS_P) reported in literature by various authors are superimposed in these plots. The parameters of these Arrhenius curves are given in Table 10.

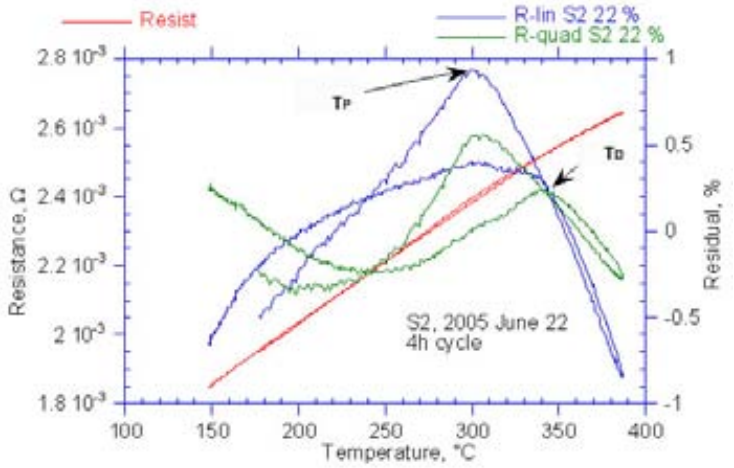

FIG. 9. Definition of T_D and T_P for the resistivity experiments (See Canadian report on the attached CD for more details).

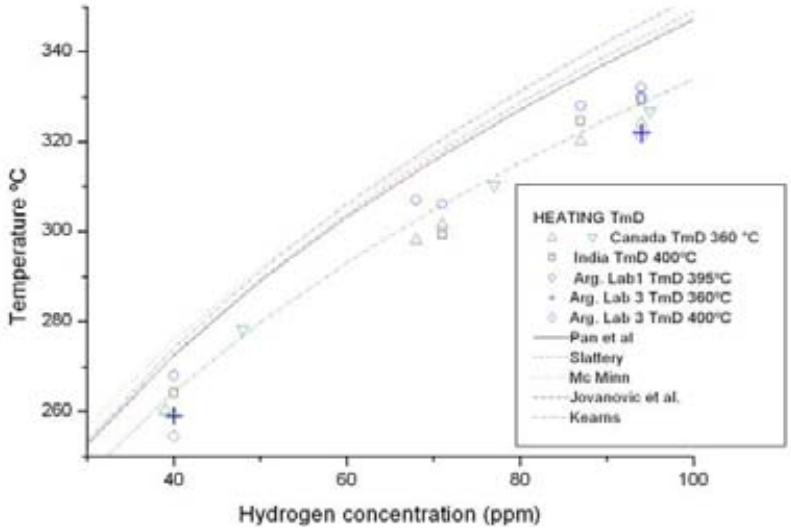

FIG. 10. T_{mD} values (Average of second and third run) measured by the participating laboratories as function of the hydrogen concentration and TSS_D curves reported in the literature.

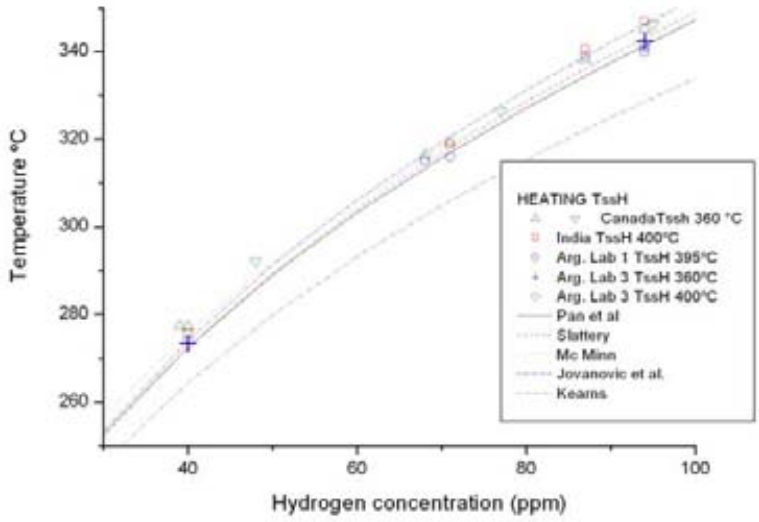

FIG. 11. T_{SSH} values (average of second and third run) measured by the participating laboratories as function of the hydrogen concentration and TSS_D curves reported in the literature.

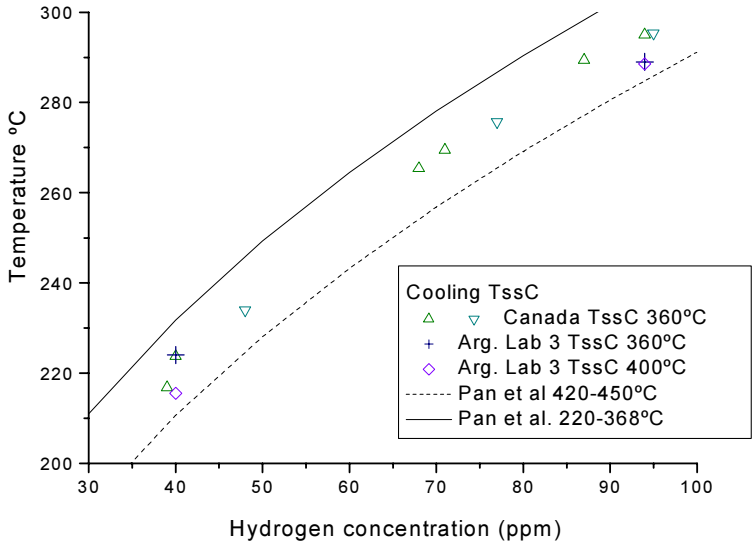

FIG. 12. T_{SSC} values (average of second and third run) measured by the participating laboratories as function of the hydrogen concentration and TSS_P curves reported in the literature.

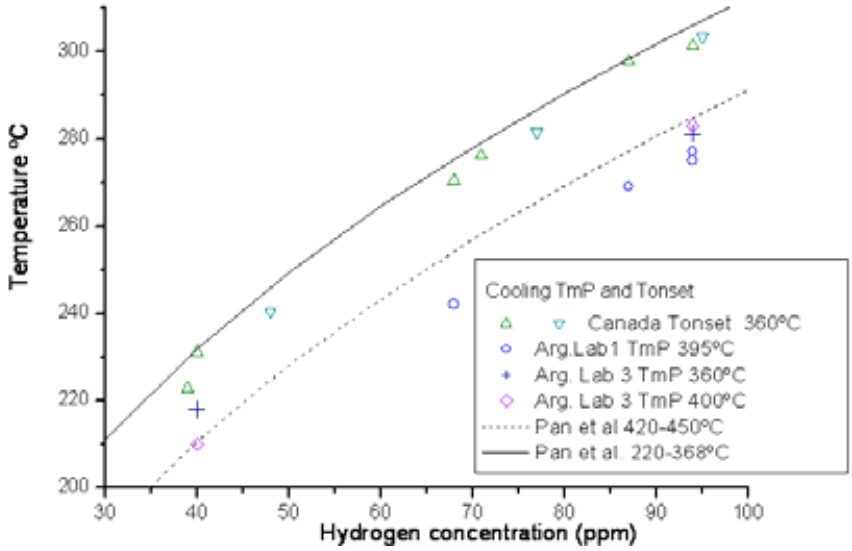

FIG. 13. T_{mP} and T_{onset} values (average of second and third run) measured by the participating laboratories as function of the hydrogen concentration and TSS_P curves reported in the literature (Pan et al. [6]*).*

2.4.3. Non-destructive examinations

Table 11 gives the results on hydrogen analysis by non-destructive examination methods. The table shows results on three sets of samples: (i) intercomparison samples, which were analyzed by Argentina, Canada and Romania-NIRDTP, (ii) samples sent to Romania-NIRDTP for NDE measurements and (iii) samples sent to Canada for NDE measurements. The expected hydrogen concentration in these samples is shown alongside.

TABLE 10. PARAMETERS FOR ARRHENIUS CURVES (TSS = A EXP(-Q/RT)) BY DIFFERENT AUTHORS DURING HYDRIDE DISSOLUTION OR PRECIPITATION TO OBTAIN HYDROGEN CONCENTRATION (R = 8.314 J/(MOL K), T (K))

Reference	Material	Method	Constants	
			A (ppmw)	*Q* (kJ/mol)
Kearns [3]	Zr	Diffusion couples	1.31×10^5	36.46
	Zry-2, Zry-4		9.87×10^4	34.53
	Three materials		1.2×10^5	35.77
Slattery [4]	Zr-2.5%Nb	Dilatometry heating	6.86×10^4	33.78
		Dilatometry cooling	4.06×10^4	27.89
Mc Minn [2]	Zry-2	DSC heating	10.64×10^4	35.99
		DSC cooling	13.87×10^4	34.47
Jovanovic et al. [5]	Zr-2.5%Nb	Equilibrium with hydrided layer heating	6.05×10^4	33.30
		cooling	4.11×10^4	28.00
Pan et al. [6]	Zr-2,5%Nb	Internal Friction heating	8.08×10^4	34.52
		Internal Friction cooling from 220-368°C	3.15×10^4	27.99
		Internal Friction Cooling from 420-450°C	2.47×10^4	25.84

TABLE 11A. RESULTS OF NDE FOR HYDROGEN DETERMINATION (INTERCOMPARISON AND ROMANIA SAMPLES)

Samples		NDE-Intercomparison				NDE-Romania			
		0-1	1-1	2-1	3-1	0-4	1-4	2-4	3-4
Measured H (ppmw) *		13±2	49±3	77±4	84±4				
Calculated H (ppmw) **						2	50	31	62
Longitudinal sound velocity [m/s]	Argentina 15 MHz	4622±8	4622±8	4616±8	4625±8	Not applicable			
	Romania-NIRDTP 10 MHz	4631±7	4631±7	4628±7	4630±7	4632±7	4633±7	4631±7	4631±7
Romania-NIRDTP Electrical conductivity 10^6 S/m		1.89	1.87 ± 0.08	1.80 ± 0.08	1.77 ± 0.08	1.89	1.80 ± 0.08	1.86 ± 0.08	1.78 ± 0.08

* HVEMS Canada, ** DSC Romania, calculated from T_{SSD} curves (see NIRDTP report on attached CD).

TABLE 11B. RESULTS OF NDE FOR HYDROGEN DETERMINATION (INTERCOMPARISON AND CANADA SAMPLES)

Samples		NDE-Intercomparison				NDE-Canada			
		0-1	1-1	2-1	3-1	0-2	1-2	2-2	3-2
Measured H (ppmw) *		13±2	49±3	77±4	84±4	3±1	48±3	77±4	95±5
Canada Electrical resistivity	$C_{H\ du}$ ppmw	-	41±10	65±8	79±6	18±15	47±10	72±8	91±10
	$C_{H\ pu}$ ppmw	15±15	35±10	60±8	81±6	24±15	44±10	79±8	103±10

* HVEMS Canada.

2.5. Assessment and discussion of results

2.5.1. Direct methods

HVE-MS method used by Canada and India performed very well for analysis of hydrogen (Tables 4 & 6 and Figures 5 & 6). The concentration measured by both the laboratories on Indian samples is very close to the expected hydrogen concentration. This not only shows the effectiveness of this technique but also reflects that the hydrogen charging process employed by India can produce samples with known amount of hydrogen concentration. The HVE-MS results from Canada on Argentinean process 1 samples show good agreement with the expected concentration. The Indian HVE-QMS results on Argentinean samples also show good agreement with the expected concentration, except for few cases. Since the technique and the process used during HVE-QMS analysis by India on these samples is identical to that used for Indian samples, it is quite likely that variation observed in analysis for some of the Argentinean samples is due to the error in labeling and/or handling. The HVE-MS results from Canada on Argentinean process 2 samples show higher values than the expected ones. After detailed assessment, Argentina concluded that there could have been some hydrogen pick-up during palladium deposition during the charging process, which was not accounted for while arriving at the expected hydrogen concentration levels. Hence, the hydrogen concentration reported by Canada using HVE-MS is considered as an expected hydrogen concentration for assessment of results on process 2 samples. It is also concluded that the process 2 employed by Argentina is not very effective to generate samples with known amount of hydrogen for such exercise.

The IGF results from Argentina Lab 1 on India samples shows good agreement for lower concentration (Table 5). The results from Argentina Lab 2 show a lower concentration than expected, even after re-calibration with a different standard. The results from Republic of Korea show a slightly higher concentration than expected. The Indian results match very closely with the expected hydrogen concentration on their sample. Similar trend is observed on Argentinean process 1 samples (Table 6).

Both the direct methods, HVE-MS and IGF performed very well for hydrogen analysis. HVE-MS showed less scatter in results obtained by different laboratories as compared to IGF (Figures 5 & 6). Although the equipment and other process details during HVE-MS analysis by India and Canada are different, their results match very closely indicating that this technique is less affected by these parameters. The lower as well as higher values than expected as reported by some laboratories using IGF are more likely to be due to some improper process parameters during analysis and is a useful feedback to these laboratories to take corrective action.

Of all the techniques attempted during this CRP, HVE-MS is the only technique that gives the isotopic composition (hydrogen and deuterium separate). This information is useful to assess the pick-up rate under reactor conditions. Results by HVE-MS and IGF are affected by any possible oxide contamination in scrape sample. Hence utmost care is required during sampling process before a sample is loaded for hydrogen analysis by these methods.

2.5.2. Indirect methods (DSC)

DSC measurements were performed by Argentina, Canada, India and Romania-NIRDTP. While Argentina and Canada performed analysis during heating and cooling cycles, India and Romania-NIRDTP made measurements during heating cycle alone. The following observations can be made on the DSC results reported by various laboratories (Tables 8a, 8b, 9a and 9b):

(a) The T_{mD} determined by all participating laboratories fall in a close range. T_{mD} values coincide well with Kearn's curve (Figure 10).

(b) T_{SSH} values reported by various laboratories show good agreement with all curves, except Kearns', which over-estimates the hydrogen concentration. Kearns´ curve was obtained by a diffusion couple and hence is not affected by the plastic deformation associated with the precipitation of hydride in the Zr-Nb matrix. It is thus expected that concentration estimated by Kearns is higher than that determined by the other authors. T_{SSH} value is better defined than T_{mD} and hence there is lower dispersion in the T_{SSH} values reported by the different laboratories.

(c) T_{SSC} values measured by Canada and Argentina are in close range (Figure 12). These values fall between the curves measured by Pan et. al. for two different temperature ranges, 420-450°C and 220-368°C. During this CRP, the dissolution temperature for determination of T_{SSC} was 360 to 400°C, which is in between the above two temperature ranges studied by Pan et. al. Hence it is expected that T_{SSC} values determined during this CRP will fall in between the two curves generated by Pan et.al.

(d) T_{onset} (measured by Canada) matches well with the Pan et.al. curve generated in the temperature range of 220-368°C. T_{mP} (measured by Argentina) matches well with the Pan et.al. curve generated in the temperature range of 420-450°C (Figure 13).

It can be concluded that T_{SSH} and T_{SSC} are better representatives for determination of the terminal solid solubility curves on heating and cooling respectively. The hydrogen assessment by indirect thermal analysis methods such as DSC and DTA depend on factors such as cell constant, gas flow rates, heating and cooling rate, etc. Specific Arrhenius relationship needs to be derived by each laboratory for the equipment and the procedure being used. However, for comparison purpose during such exercise, the analysis parameters (gas flow rate, heating and cooling rate, dissolution temperature) need to be identical for all the laboratories.

2.5.3. Non-destructive examination (NDE) methods

Three NDE methods were attempted for hydrogen analysis during this CRP: (i) ultrasonic testing based on sound velocity measurement, (ii) eddy current testing based on conductivity measurement and (iii) resistivity based measurement. While ultrasonics and eddy current testing were employed at room temperature under static conditions, the resistivity-based measurements were performed under dynamic conditions during heating and cooling.

The sound velocity measurements performed by Argentina and Romania-NIRDTP do not show significant change with the increase in hydrogen concentration. Argentinean experience shows that a significant change in sound velocity is observed at a much higher hydrogen concentration (few hundreds of ppm [7]). Hence, at this stage static ultrasonic velocity measurement is not found to be a suitable method for determining hydrogen concentration in the range of 0 to 100 ppm. The same also applies for static conductivity measurement using eddy current for the hydrogen concentration of less than 100 ppm. Better results with eddy current are expected to be obtained with a focused transducer. Data analysis using neural network may also help.

Resistivity-based measurement employed by Canada has emerged as the most promising NDE method for hydrogen analysis. The hydrogen concentrations reported by Canada using resistivity-based measurement are very close to expected values. It is noteworthy that the technique is not only sensitive to hydrogen concentration of interest (<100 ppm) but is also able to differentiate between varying levels of hydrogen in the range of 0-100 ppm.

3. BLISTER CHARACTERIZATION

3.1. Contributions from participating laboratories

3.1.1. Argentina

Argentina prepared blister samples for round robin analysis. The PT sections were charged with controlled amount of hydrogen and subjected to homogenization annealing treatment before loading it into the blister generation set-up. In this set-up, the PT sample is heated internally and a cold spot is created on the outside surface of PT by a water-cooled metallic block. Four PT sections (two containing two blisters and the remaining two containing one blister) were prepared.

Argentina employed eddy current and ultrasonic testing for detection of hydride blister. Eddy current technique was used from outside surface and hence will not be applicable for in-situ assessment of PT. However, this technique can be employed during post-irradiation examination of PTs for blister detection. Ultrasonic technique was employed from inside as applicable during in-service inspection. Ultrasonic testing was carried out using four angle beam shear wave transducers.

3.1.2. Canada

Canada examined the two PT sections containing blisters. Ultrasonic testing using angle beam shear wave and normal beam longitudinal wave was carried out.

3.1.3. Romania-NIRDTP

Romania-NIRDTP examined four PT sections containing blisters using eddy current technique. This was carried out from inside surface as applicable during in-service inspection. Since the PT samples on which blisters were generated have small lengths, the inner eddy current transducer with rotating magnetic field could not be used for this study. Therefore, an eddy current transducer with orthogonal coils in the send-receive mode was used.

3.1.4. Romania-NNDT

Romania-NNDT examined four PT sections containing hydride blisters. NNDT used ultrasonics for blister detection and characterization. Both, angle beam shear wave and normal beam longitudinal waves, were used for examination. Ultrasonic C scan images were collected during examination.

India and Republic of Korea

India and Republic of Korea did not receive the PT samples containing blisters.

3.2. Sample Preparation

3.2.1. Materials and samples

Argentina generated hydride blisters on four un-irradiated Zr-2.5% Nb PT samples for round-robin analysis. Two of these PT sections (each approximately 160 mm long) were made from the Canadian PT sample and the remaining two sections (each approximately 100 mm long) were made from the CANDU PT of Argentinean HWR, Embalse. The samples are labelled as follows:

C1: Canadian PT, 2 blisters, a and b
C2: Canadian PT, 2 blisters, a and b
A1: Argentinean PT, 1 blister
A2: Argentinean PT, 1 blister

3.2.2. Blister formation

The blister generation on a pressure tube samples involved the following three steps:

(a) Hydriding by cathodic charging,

(b) Homogenization annealing,

(c) Diffusion of hydrogen to cold spot under thermal gradient.

3.2.2.1. Hydriding by cathodic charging:

The PT samples used during this CRP contain some initial hydrogen of the order of few ppm. However, in order to accelerate the blister formation process, the PT sections were hydrided to approximately 100 ppm of hydrogen. The hydriding operation was carried out by an electrolytic method on the inner surface of the tube without removing the surface oxide. Annular sections ~25 mm long were charged with hydrogen (Figure 14). The details of the hydriding process are described below.

The PT sample is placed in the vertical position in an electrolytic charging set-up and refrigerated with flowing water. The section chosen to be hydrided was sealed with two Teflon plugs (Figure 15) to avoid electrolyte leak. The upper plug has two holes, one for the lead anode and the other for the thermocouple and a connection to an exhaust line and steam condenser.

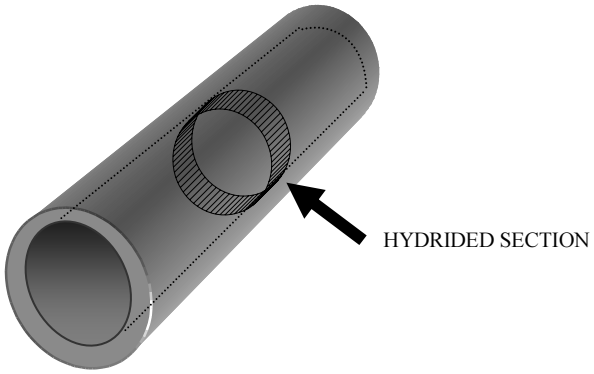

FIG. 14. Section of the pressure tube showing the hydrided layer.

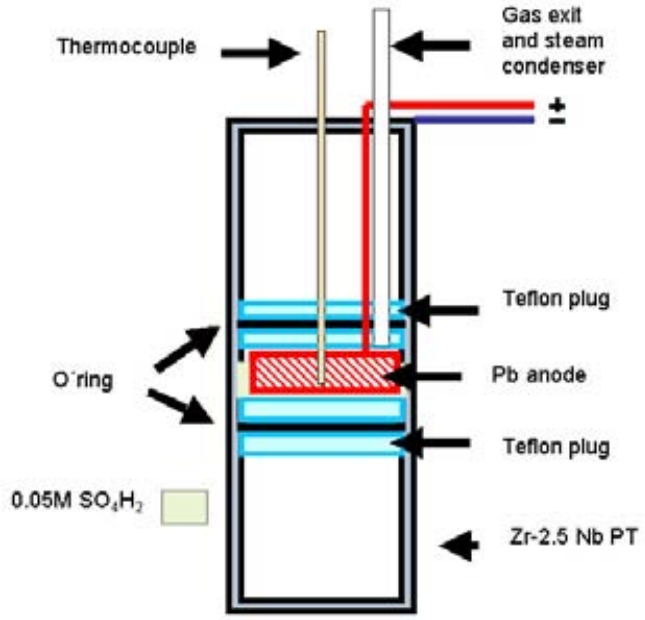

FIG. 15. Electrolytic hydriding rig.

The hydriding was carried out under the following conditions

- Anode: Pb
- Electrolyte: 0.05M H_2 SO_4
- Current density: 210-250 mA/cm^2
- Temperature: 70-95°C

During electrolytic charging a hydride layer is formed on the sample surface. The thickness × of this layer is calculated taking into account that: the hydrogen mass contained in it ($m_H^{hydride}$) will be redistributed in the sample bulk (m_H^{alloy}) during a subsequent heat treatment, in order to produce the expected hydrogen concentration in the sample (C_H).

Hydrogen concentration of the hydride layer before heat treatment is:

$$C_H^{hydride} = \frac{m_H^{hydride}}{(m_H^{hydride} + V_{hydride} \cdot \rho_{hydride})} 10^6 \; ppm = 16000 \, ppm \qquad (1)$$

Where, $V_{hydride}$ = volume of the hydride layer
= A·x, (2)
A is the area exposed to the electrolytic solution, x is the layer thickness.

Hydrogen concentration of the sample after heat treatment is:

$$C_H^{alloy} = \frac{m_H^{alloy}}{(m_H^{alloy} + V_{alloy} \cdot \rho_{alloy})} 10^6 \; ppm \tag{3}$$

Where, V_{alloy} = volume of the PT section hydrogenated
= A·e, (4)
e is the thickness of PT sample (4 mm).

Making a balance mass between $m_H^{hydride}$ and m_H^{alloy}, the thickness of the hydride layer may be calculated as:

$$x = \frac{e \cdot C_H \cdot \rho_{Zr} \cdot (10^6 - 16000)}{(10^6 - C_H) \cdot \rho_{ZrH_{1.6}} 16000} \tag{5}$$

where, C_H is the hydrogen concentration,
ρ_{zr} is the Zirconium density (6.49 g/cm^3),
$\rho_{zrH1.6}$ is the Hydride density (5.65 g/cm^3).

The time t required for obtaining the hydride layer of thickness x by hydriding is evaluated with Sawatzky equations [8].

$$x = 0.85\sqrt{Dt} \tag{6}$$

$$D = 3.23 \cdot 10^{-5} \exp(-9700/1.987T) \tag{7}$$

where, D is the diffusion coefficient of hydrogen in the hydride
T is the temperature in Kelvin.

Although, Equations 6 and 7 are valid for Zircaloy-2, the Argentinean experience shows that when these are applied to Zr-2.5% Nb, hydride layer thickness obtained is 1.5-3 times thicker than the layers produced in Zircaloys. This is due to the higher diffusion coefficient of hydrogen in the Zr-2.5% Nb (due to β phase) as compared to Zircaloy-2. Considering this fact one can arrive at the following:

$$1.5 \times 0.85\sqrt{Dt} \le x_{Zr\text{-}2.5Nb} \le 3 \times 0.85\sqrt{Dt} \tag{8}$$

It is important that the hydrided layer produced during charging process is completely dissolved during subsequent annealing. In order to preserve the mechanical properties and microstructure of the PT, the annealing temperature must not exceed 400ºC. This temperature determines the maximum hydrogen content C_H that can be introduced by cathodic charging and thereby the maximum thickness of hydride layer.

According to Jovanovic [5], the solubility of hydrogen in Zr-2.5%Nb is given by:

$$C_H = 60500 \exp(-33300/(8.314T)) \tag{9}$$

where, T is the temperature in Kelvin.

At 400ºC, the C_H comes to 157 ppm. This puts a limit of 47 μm on the thickness of hydrided layer ($x_{Zr\text{-}2.5\%\ Nb}$) that can be produced in Zr-2.5% Nb PT.

As the PT sample cannot be cut to verify the formation of hydride layer, a control sample of 4 mm × 4 mm, cut from a Zr-2.5%Nb PT, was charged under similar conditions. The external surface and the edges of this sample were painted to avoid hydriding. The thickness of the hydride layer after cathodic charging as measured by optical microscopy was found to be 26 μm. It is assumed that a layer of similar thickness is also formed on the inside surface of the PT sections used for blister generation.

3.2.2.2. Homogenization annealing.

The objective of homogenization annealing is to dissolve the hydride layer formed on the inside surface of the PT section during the cathodic charging process. An electrical heating coil was introduced inside the PT section (Figure 16) while the outside surface was wrapped with a ceramic blanket. The temperature was measured at two points, with thermocouples placed between the PT and the furnace. The temperature along the length of PT was found to vary between 385–410 ºC. The time (t) required for homogenization treatment was calculated as:

$$t = e^2 / D \ [8] \tag{10}$$

$$D = 3.8 \cdot 10^{-3} \exp(-38580/8.314 \cdot T)(cm^2 / s) \tag{11}$$

where, D is the diffusion coefficient reported by Skinner and Dutton [10],
T is the temperature in K,
e is the PT thickness (4 mm).

At 400 ºC, the time required to achieve homogenization across the PT thickness was calculated to be 13 hours. The time and temperature during the homogenization treatment for the four PT sections are given in the Table 12. Longer times were used to assure complete dissolution of hydride layer.

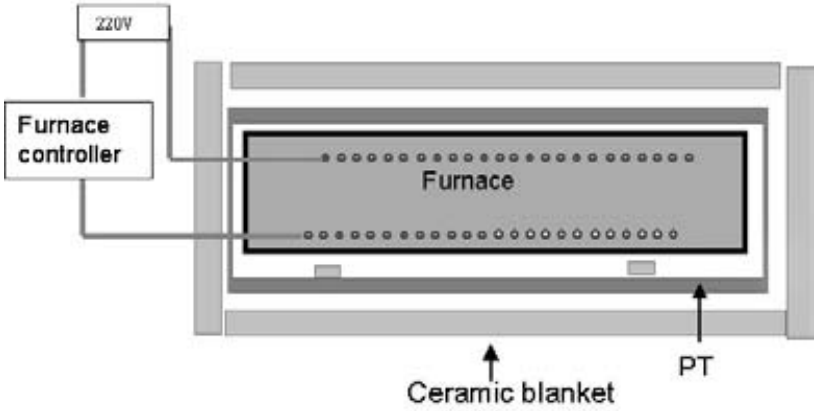

FIG. 16. Experimental device for homogenization annealing.

TABLE 12. PT HOMOGENIZATION, TIME AND TEMPERATURE

SAMPLE	Temperature (ºC)	Duration (hr)
A1	370-380	50
A2	380-403	38
C1	380-408	85
C2	370-400	32

3.2.2.3. Hydrogen diffusion under thermal gradient

To generate a hydride blister, a thermal gradient is created at a localized zone, by internally heating the PT section and creating a cold spot on the outside surface. Figure 17 shows a schematic of the set-up employed to produce the thermal gradient. A water refrigerated aluminum block is pressed on the sample by means of a spring. One of the blocks had a circular tip (diameter = 2mm), and the other one had a rectangular tip (2 mm in the circumferential direction and 5 mm in the axial direction). The PT sections were left under this thermal gradient for a period of 20 days to generate hydride blister at the cold spot(s). The photographs of the blisters generated in four PT sections are shown in Figures 18, 19 and 20.

3.3. Blister detection and characterization techniques

Four PT sections with hydride blisters were sent to different laboratories for non-destructive evaluation. These samples were examined by Argentina, Canada, Romania (NIRDTP) and Romania (NNDT). The blister samples could not be examined by India and Republic of Korea.

This section gives the account of various NDT methods employed by participating laboratories for detection of hydride blisters in PT samples. Table 13 summarizes the NDE methods employed by participating laboratories for blister characterization during this CRP:

3.3.1. Argentina

Argentina employed ultrasonic testing (UT) and eddy current testing (ET). While UT was carried out from the inside surface, ET was performed from the outside surface. Since the outside surface of PT is not accessible during in-service inspection, ET technique employed by Argentina cannot be used for in-situ assessment of pressure tubes. However, it can be applied during post irradiation examination.

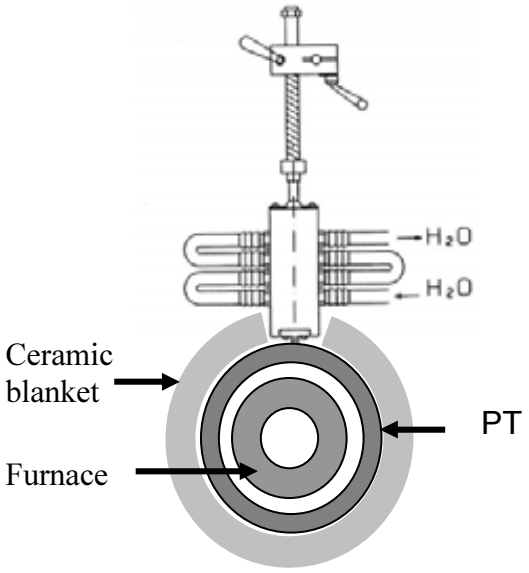

FIG. 17. Blister generation set-up.

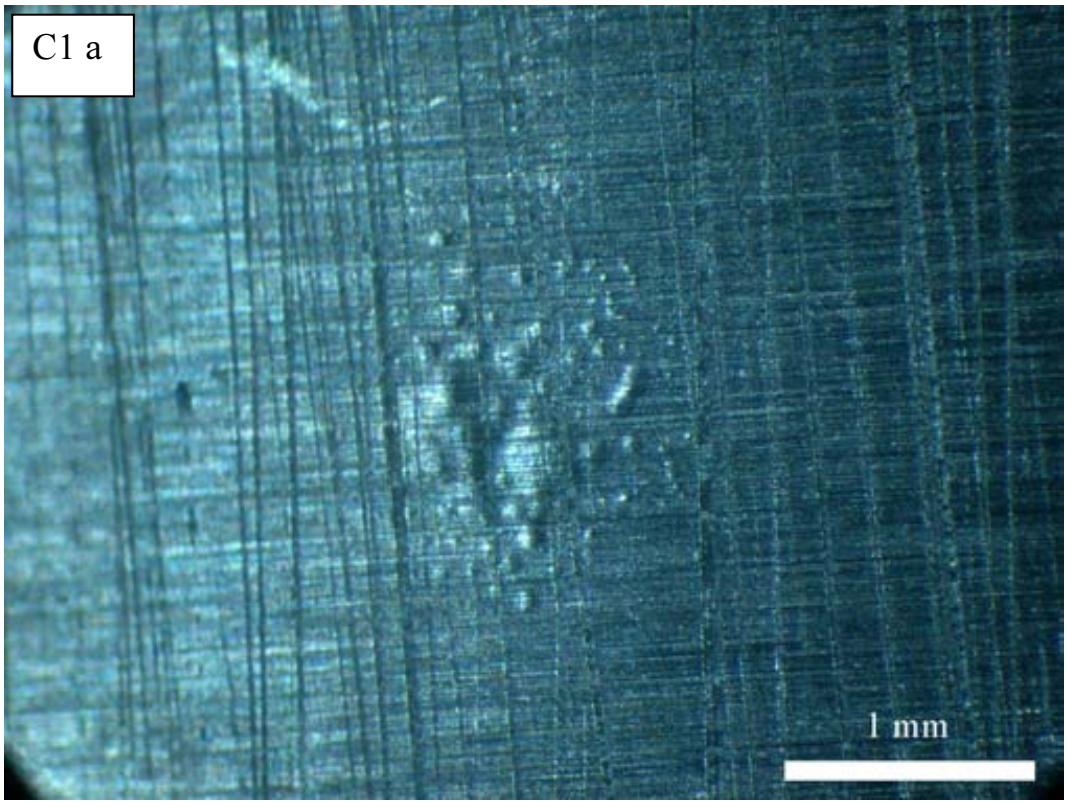

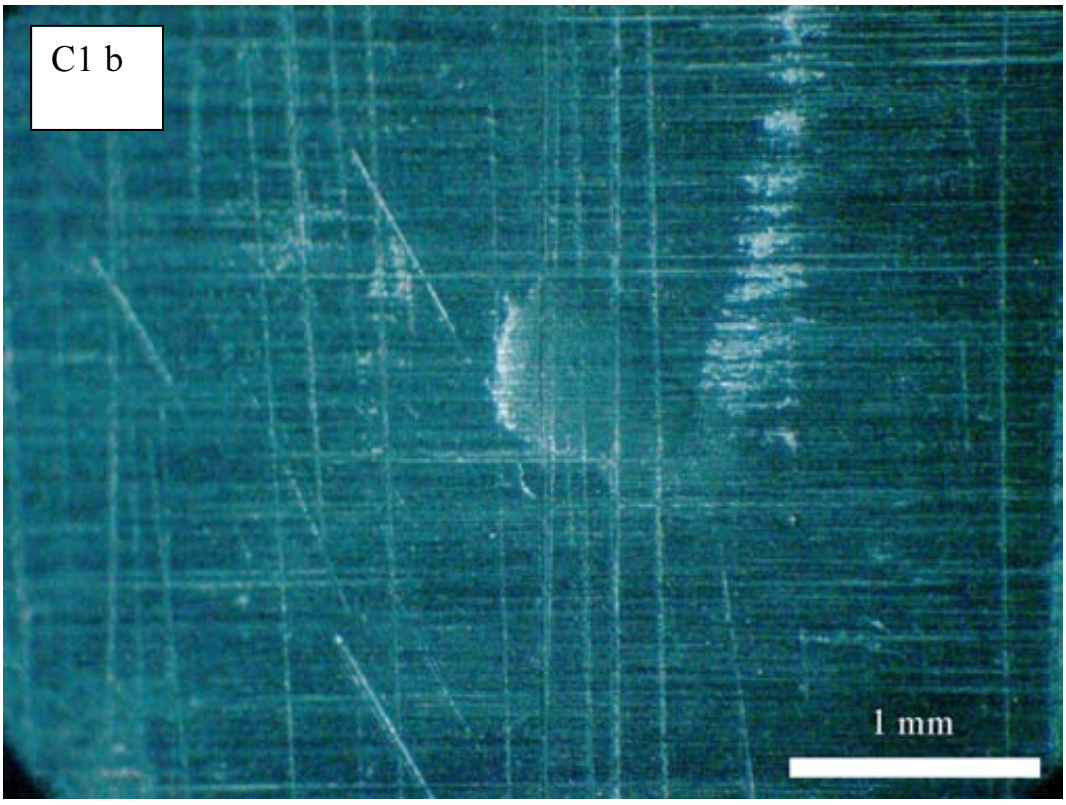

FIG. 18: Blisters a and b in C1.

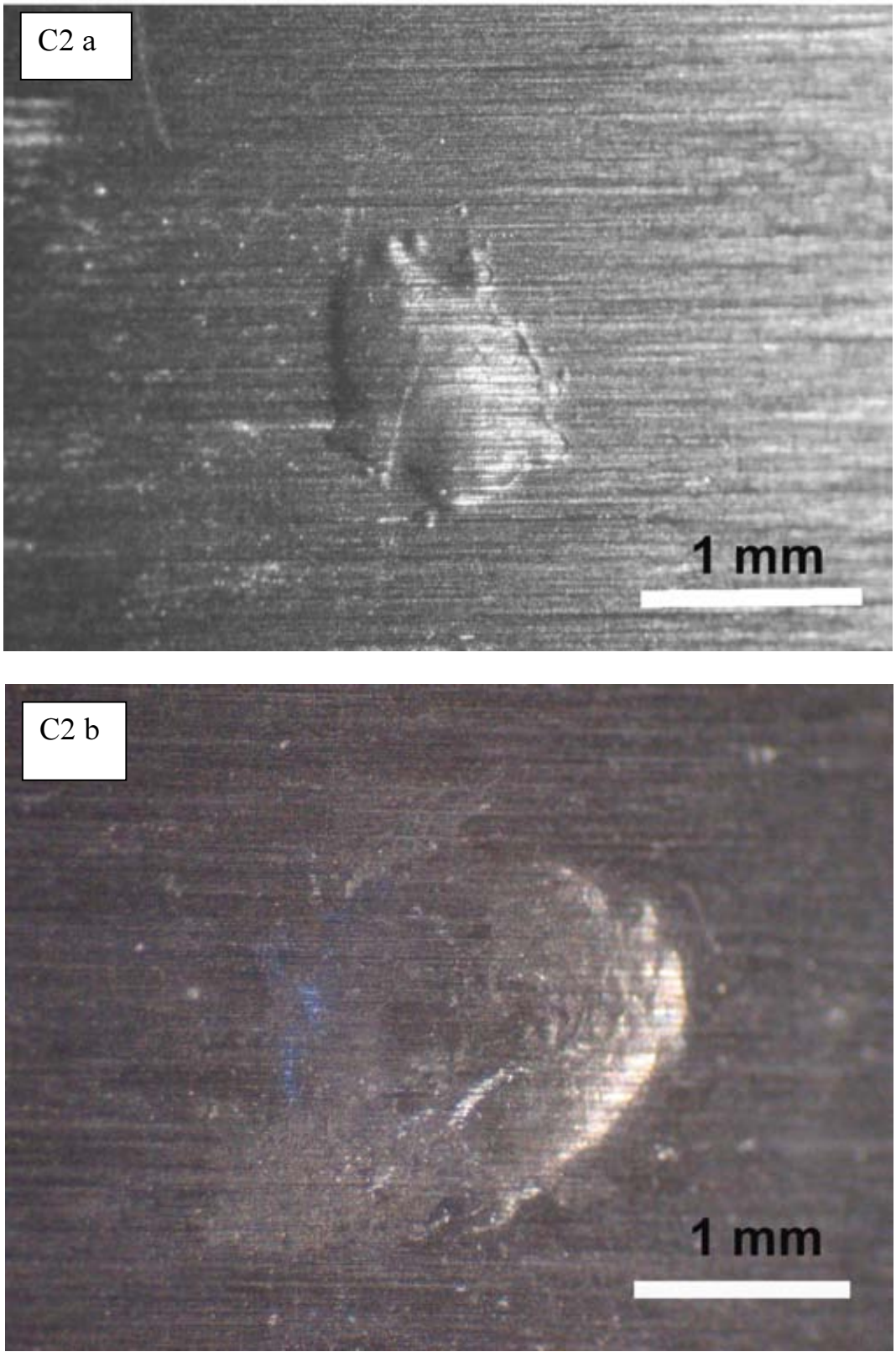

FIG. 19. Blisters a and b in C2.

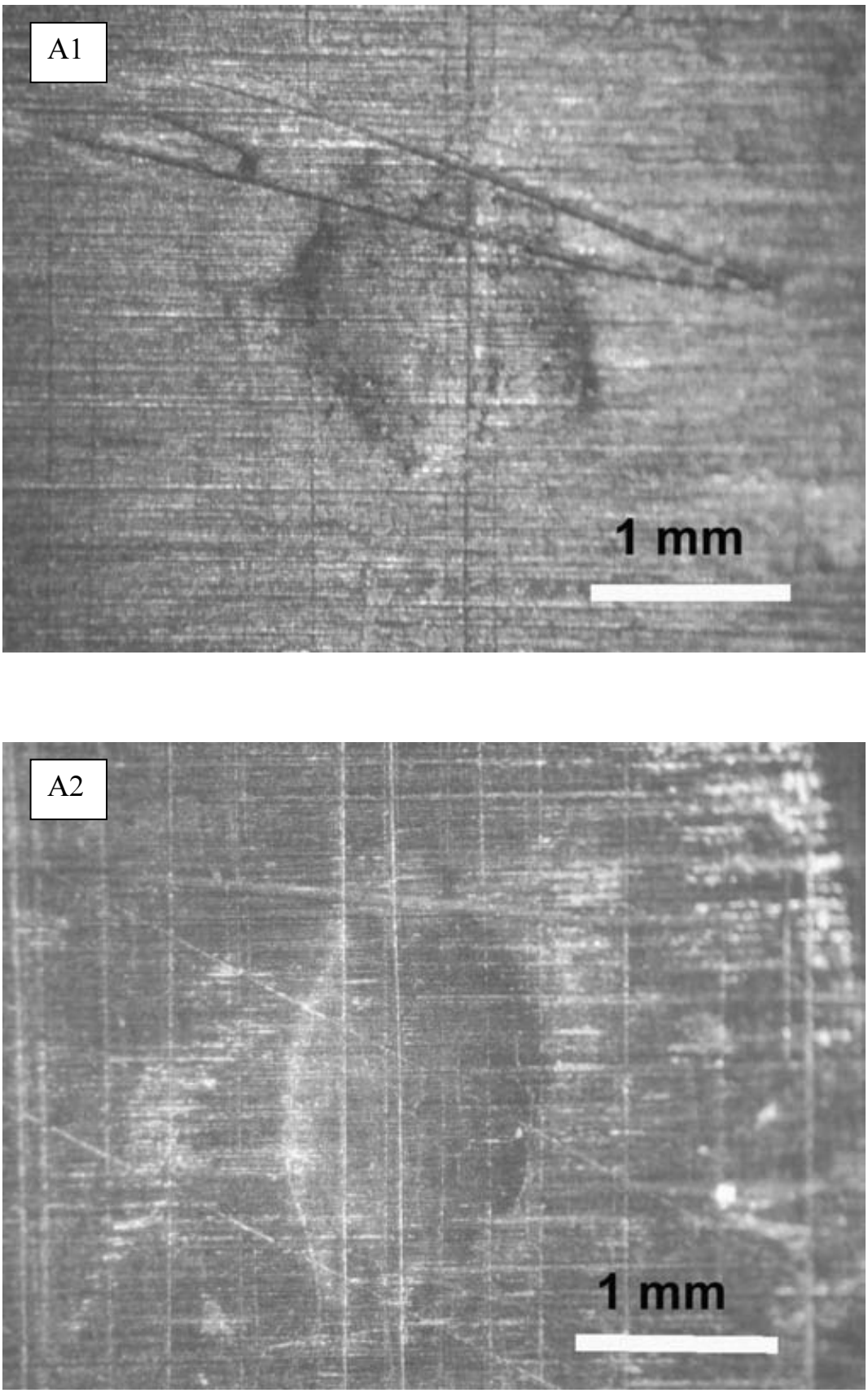

FIG. 20. Blisters in PT samples A1 and A2.

TABLE 13. NDE METHODS FOR BLISTER CHARACTERIZATION

Participating Laboratory	Ultrasonic Testing	Eddy Current Testing
CNEA, Argentina	x	x
AECL, Canada	x	-
NIRDTP, Romania	-	x
NNDT, Romania	x	-

3.3.1.1. Ultrasonic testing

Ultrasonic testing was carried out using four angle beam shear wave probes, two looking axially while the other two looking circumferentially. Reference notches on the inside and outside surface of pressure tube sample made as per CAN CSA N285.4 [11] (6 mm long, 0.15 mm wide, 0.15 mm deep) are used for calibration. C scan images were collected during the examination.

3.3.1.2. Eddy current

Eddy current tests were performed from the inner and outer surfaces of the PT at different frequencies in the impedance mode with specially tailored curved probes made from rectangular planar coils. For zircaloys, the inspection frequency of 9 kHz corresponds to the standard depth of penetration of 4.5 mm, which is equal to the wall thickness of PT. Hence tests were made at frequencies in the range 3.0 to 30 kHz.

3.3.2. Canada

Canada withdrew from this task of this CRP, however did inspect PT samples A1 and A2 by UT using the techniques applicable for flaw detection. UT was carried out using both, angle beam shear waves and normal beam. Reference notches on the inside and outside surface of pressure tube sample made as per CAN CSA N285.4 (6 mm long, 0.15 mm wide, 0.15 mm deep) are used for calibration during angle beam examination. C scan images were collected during scanning.

3.3.3. Romania-NIRDTP

Romania-NIRDTP employed ET for detection of hydride blisters. This examination was performed from the inside surface. The four PT samples containing blisters were too short to use the inner eddy current transducer with rotating magnetic field. Hence, an ET transducer with orthogonal coils in the send-receive mode was used for PT examination. The detailed account of ET transducer used for this study is given in Romania-NIRDTP report (attached CD). The testing parameters during blister detection are given below:

Frequency 40 kHz, Gain 49 dB, Injection $0.1A_{ef}$, Phase 178^0, Cut-off freq. 20Hz

3.3.4. Romania-NNDT

Romania-NNDT employed ultrasonic testing for detection of hydride blister in the four PT sections. The examination involved angle beam scanning and normal beam scanning of the PT samples. Angle beam examination was carried out in both pulse-echo (reflection) mode as well as pitch-catch (transmission) mode in axial and circumferential directions. For angle beam scanning, calibration was

performed using reference notches on the inside and outside surface of pressure tube sample made as per CAN CSA N285.4 (6 mm long × 0.15 mm wide × 0.15 mm deep).

During angle beam pulse-echo examination, the blister detection was based on monitoring the reflected signal as in the case of flaw detection. In pitch-catch and normal beam scans the blister detection was based on the drop in the amplitude of the transmitted signal and back wall signal respectively. In addition to the amplitude drop, the time-of-flight of the backwall was also monitored during normal beam examination. C scan images based on amplitude and time-of-flight were collected during angle beam and normal beam scans. The inspection head contains four 10 MHz transducers for angle beam (45º shear waves, double skip / W pattern, one pair looking axially and the other looking circumferentially) and normal beam transducers (10 MHz, 25 MHz and 50 MHz, focused on outside surface).

Romania-NNDT has also developed UT technique using Lamb waves for detection and characterization of hydride blisters in PT. The four PT samples containing blisters were examined by this technique. Additional research work on signals processing and interpretation procedure is underway.

India and Republic of Korea

India and Republic of Korea did not receive blister samples and hence could not produce any results on PT sections circulated as part of this CRP. Both these laboratories have carried out extensive research on blister detection using ultrasonics on samples generated in-house. India has standardized UT techniques based on velocity ratio measurement, B & C scan imaging and amplitude drop monitoring near critical angle. Republic of Korea has standardized UT technique based on B & C scan imaging using several parameters such as time-of-flight, amplitude and velocity ratio.

3.4. Experimental results

3.4.1. Argentina

Ultrasonic angle beam examination detected all the blisters in samples C1, C2, A1 and A2. The amplitude of the signals obtained from blisters during angle beam examination is found be lower than the reference standards. The signal to noise ratio was also poor for blisters in PT samples A1 and A2 as compared in C1 and C2. The C scan images for some of the blisters are in Figure 21.

Eddy current tests from inside surface could not detect any blister. The inspection from the outside surface of PT however showed distinct signals from blisters in all the PT samples. The signal amplitudes were however rather low and the Z-plane indications (X-Y mode) were not all that clear. Better detection was achieved in the X-t; Y-t mode. The signals at 270 kHz are shown in Figure 22. The best indications are observed from blisters in samples C1 and C2. The indications of blister *a* in tube C1 (Fig. 22a) are less prominent and more difficult to analyze than those from blister *b* in tube C2 (Fig. 22b). During the eddy current tests of PT samples A1 and A2, the signals from blister were slightly higher than the signals produced by noise, lift-off and surface imperfections. This was not the case with the PT samples C1 and C2. This difference may be due to the presence of scratches and imperfections on the surface of tubes A1 and A2 in the blister zone. Detailed results from eddy current measurements are given in Argentinean report in attached CD.

Blister A2

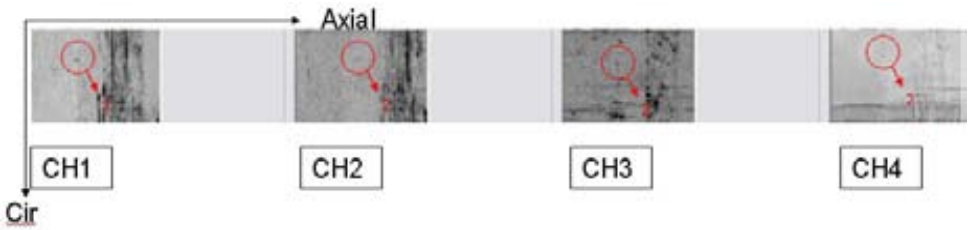

Gain CH1: 54dB Gain CH2: 54dB Gain CH3: 54dB Gain CH4: 50dB

FIG. 21a. C scans for blister A2.

Blister C2-*b*

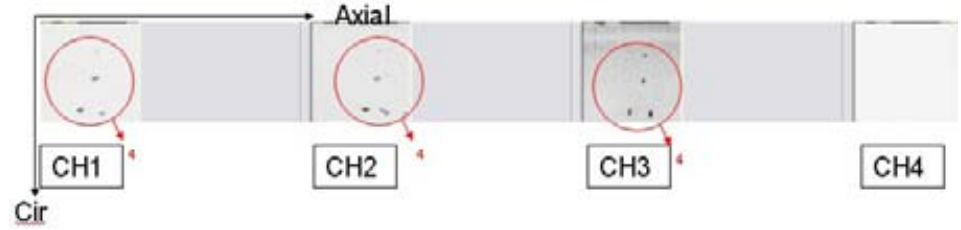

Gain CH1: 45 dB Gain CH2: 45 dB Not working Gain CH3: 45 dB Gain CH4:

FIG. 21b. C scans for blister C2-b.

Blister C1-a

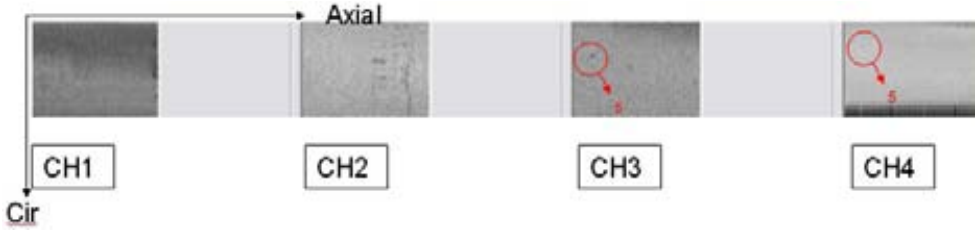

Gain CH1: 58dB Gain CH2: 52dB Gain CH3: 52dB Gain CH4: 52dB

FIG. 21c. C scans for blister C1-a.

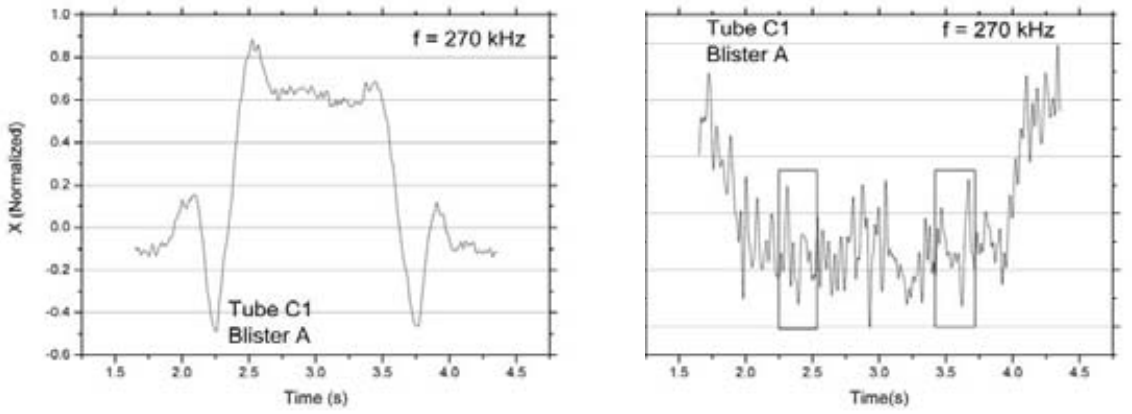

FIG. 22a. Eddy currents X(t), Y(t) signals for blister a in C1.

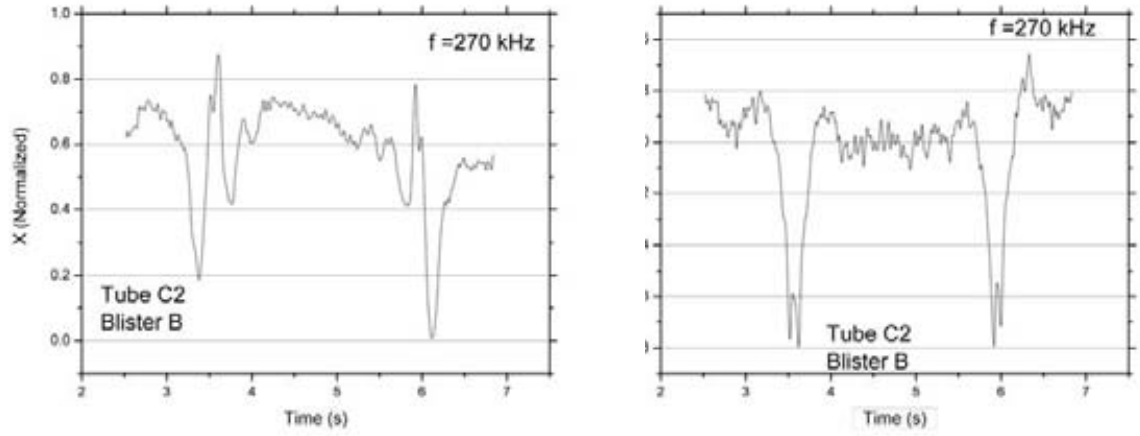

FIG. 22b. Eddy eurrents X(t), Y(t) signals for blister b in C2.

3.4.2. Canada

The two blisters were detected by angle beam shear wave examination, though the standard flaw detection technique could not differentiate whether the indications corresponded to a crack within the blisters or the geometry change associated with blister formation. Signal to noise ratio was rather low. The signal amplitude from the blister in tube A1 is higher than that from tube A2, probably showing that the former was in a more advanced stage of development than the latter. Normal beam examination could not detect the blisters.

3.4.3. Romania-NIRDTP

Signals from all the blisters were detected, though their characteristics differ greatly. Signal-to-noise ratio was rather low except for the blister in tube A1 and blister *a* in tube C2. The ET results are presented in Table 14. Some of the plots are shown in Figure 23. Detailed results can be found in Romania-NIRDTP report (attached CD).

TABLE 14. ET SIGNAL CHARACTERISTICS ON BLISTERS

Blister	Channel X [mV]	Channel Y [mV]	Signal-to-Noise Ratio
A1	171	185	8:1
A2	28.5	25	3:1
C1*a*	42.8	17.8	1.5:1
C1*b*	21.4	64.2	3.5:1
C2*a*	50	196	8:1
C2*b*	85	67.8	Difficult to evaluate

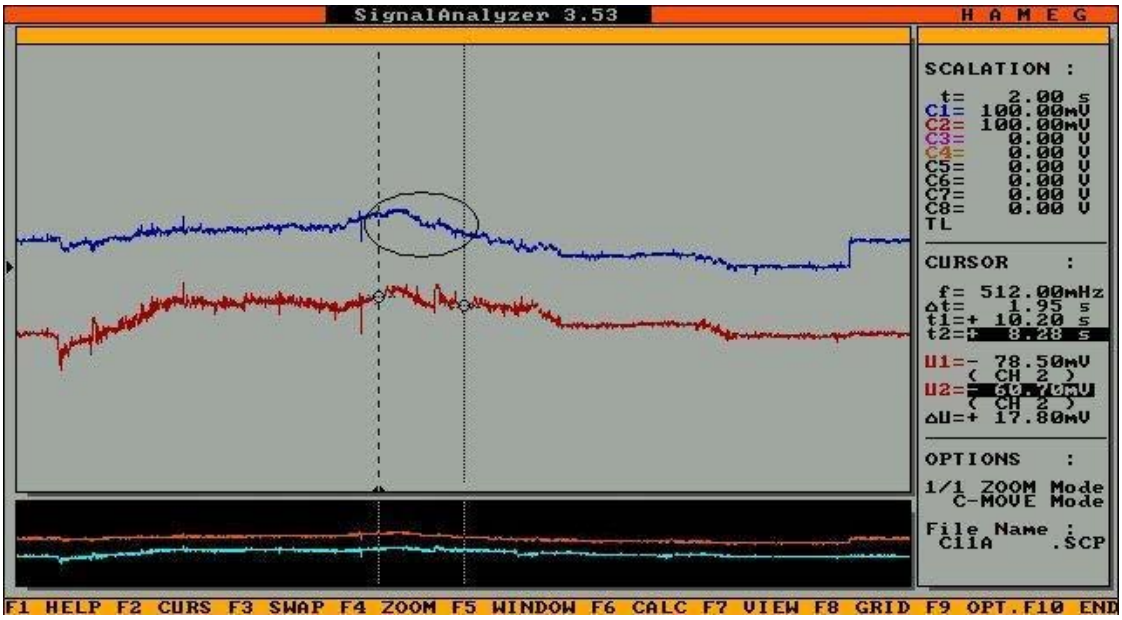

FIG. 23a. Eddy current signal from blister C1-a.

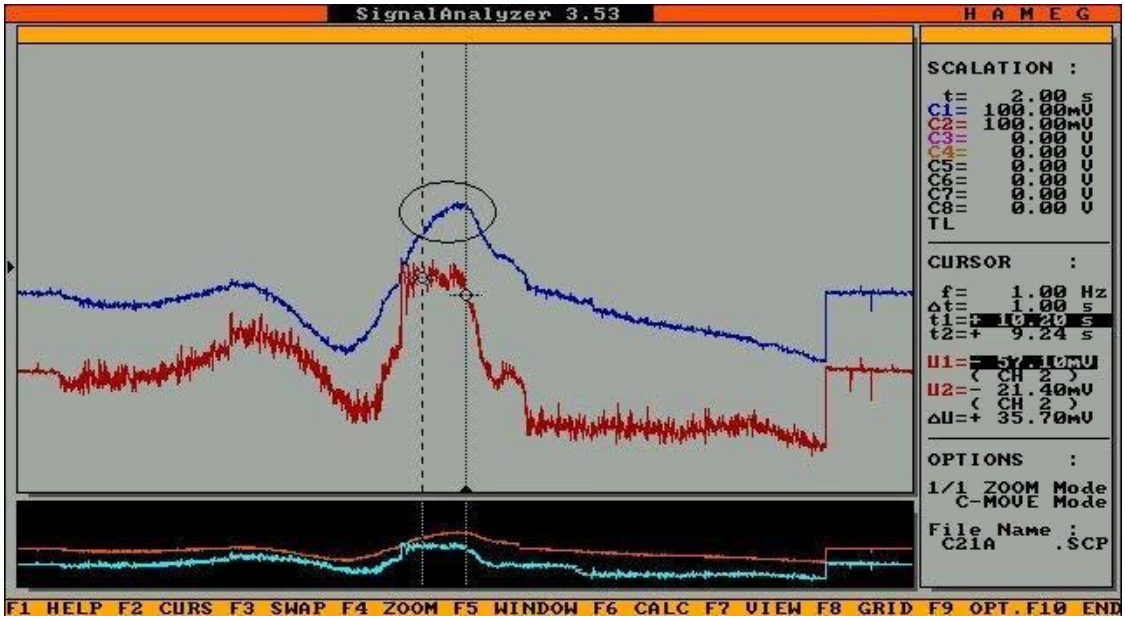

FIG. 23b. Eddy current signal from blister C2-a.

3.4.4. Romania-NNDT

The results on ultrasonic examination on PT samples for blister detection are given in Table 15 and Table 16. Table 15 deals with results of angle beam and normal beam examination and Table 16 gives signal characteristics observed during angle beam pulse-echo examination.

Table 16 summarizes the amplitude of reflected shear wave signals (A / SWA and C / SWC examination modes) observed during pulse-echo angle beam examination during axial and circumferential scans.

TABLE 15. ULTRASONIC TESTING RESULTS ON BLISTER SAMPLES

Blister ID	Examination Mode	Amplitude [%]	Length [mm]	Standard Width [mm]	Remarks
A1	NA / BWD1	9.8	0.65	0.69	50 MHz transducer
	NA / BWD2	12.4	0.56	0.41	25 MHz transducer
	PC / SWPC1	64.5 65.1	1.93 1.50	1.83 1.84	-
	C / SWC1	13.2	-	-	-
A2	NA / BWD1	18.3	0.42	0.29	50 MHz transducer
	NA / BWD2	28.4	0.66	0.41	25 MHz transducer
	PC / SWPC1	63.5 68.8	1.72 1.40	1.36 1.24	-
	C / SWC1	33.4	-	-	-
	C / SWC2	15.6	-	-	-
	PA / SWPA2	41.8 53.5	-	-	-
	A / SWA1	29.2	-	-	-
	A / SWA2	12.8	-	-	-
C1*b*	NA / BWD1	31.9	0.92	0.71	50 MHz transducer
	NA / BWD3	15.9	0.54	0.68	25 MHz transducer
	C / SWPC1	37.0 38.9	1.04 0.94	1.07 0.89	-
	C / SWC1	34.0	-	-	-
C1*a*	NA / BWD2 & 4	-	-	-	Not detected
	A, C	-	-	-	Not detected
	PC / SWPC3	-	-	-	Not detected
C2*b*	NA / BWD1	100	1.11	0.71	50 MHz transducer
	NA / BWD6	84.7	1.24	0.78	50 MHz transducer
	NA / BWD7	54.2	1.81	2.49	10 MHz transducer
	PC / SWPC5	81.1 75.8	1.96 1.96	1.81 1.80	-
	C / SWC1	95.8	1.39	1.28	-
C2*a*	NA / BWD2&5&8	-	-	-	Not detected
	A	-	-	-	Not detected
	C / SWC1	-	-	-	Not detected
	PC / SWPC4	36.8	1.04	0.99	-

Notes: Refer to Romania-NNDT report (attached CD) for more details

- BWD: Normal beam backwall drop;
- SWPC/SWPA: amplitude drop in pitch-catch mode (Circumferential/Axial);
- SWC/SWA: reflected signal amplitude in pulse-echo (Circumferential/Axial).

TABLE 16. ULTRASONIC TESTING RESULTS ON BLISTER SAMPLES: ANGLE BEAM PULSE-ECHO

Blister ID	Examination	Amplitude (% Ref)	Characterization
A1	SWC1	14.6	Possible reflection from scratches
A2	SWC1	37.1	Possible reflection from scratches
	SWC2	17.3	Possible reflection from scratches
	SWA1	32.4	Possible reflection from scratches
	SWA2	14.2	Possible reflection from scratches
C1*b*	SWC1	37.7	Possible reflection from scratches
C1*a*	SWC1	-	No reflection from blister
C2*b*	SWC1	106.4	Possible cracks in blister
C2*a*	SWC1	-	No reflection from blister

The best results were obtained using the shear wave pitch-catch technique in circumferential mode (PC). Using this method, a significant transmitted echo amplitude drop was observed for five out of the total six blisters in all samples. Only blister *a* from C1 sample was not detected. Good results were also obtained by backwall echo acquisition using high frequency normal beam transducers. Significant backwall drop was observed for the blister *b* in C2 sample. Blisters from A1 and A2 samples, and blister *b* from C1 although detected, did not show a significant backwall drop. Blister *a* in C1 and C2 could not be detected by normal beam examination. During angle beam pulse-echo examination, except for blister C2-*b*, the amplitudes of reflected signals are much smaller than the amplitude from the calibration notches made as per CAN-CSA N285.4 [11].

Figures 24a to 24e show the amplitude based C scan images obtained with the circumferential angle beam pitch-catch (PC) technique. This technique also gives a good estimate of blisters dimensions in the circumferential-axial plane. Since the blisters are on the outside surface, the ultrasonic beam intercepts the blister twice because of the double skip (W-pattern) employed in the shear wave pitch-catch mode. As a result the C scan image shows two indications from the same blister. The normal beam amplitude drop C scan image of one blister (C2-*b*) is shown in Figure 25. It can be seen the blister dimensions in the circumferential-axial plane evaluated from normal beam amplitude drop are significantly smaller as compared to the one evaluated by shear wave pitch-catch technique. The blisters depths could not be evaluated by any of the above techniques.

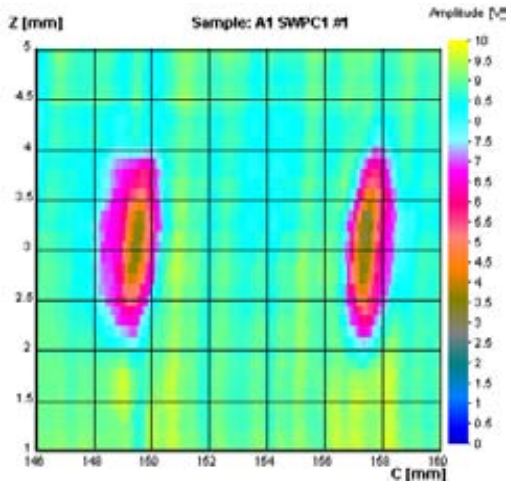

FIG 24a. PC amplitude image of the blister A1.

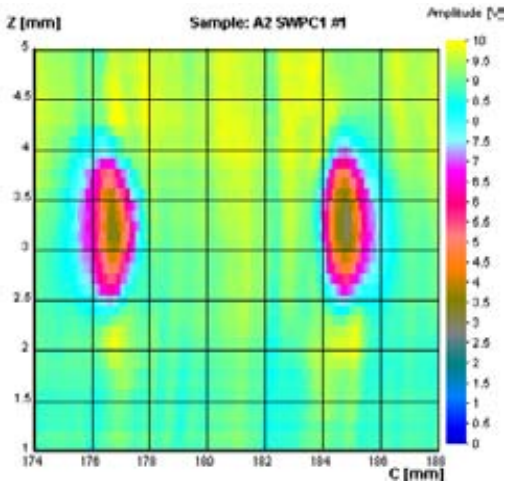

FIG. 24b. PC amplitude image of the blister A2.

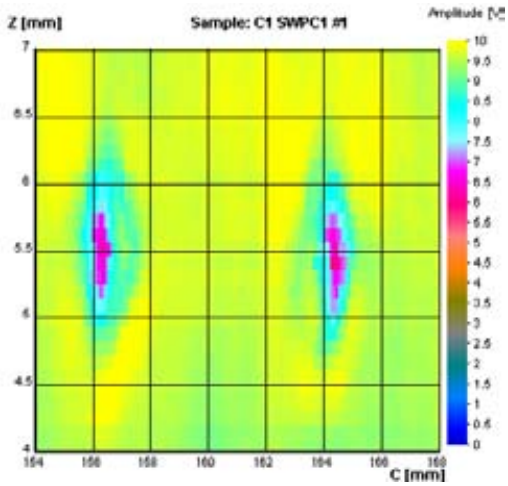

FIG. 24c. PC amplitude image of the blister C1-b.

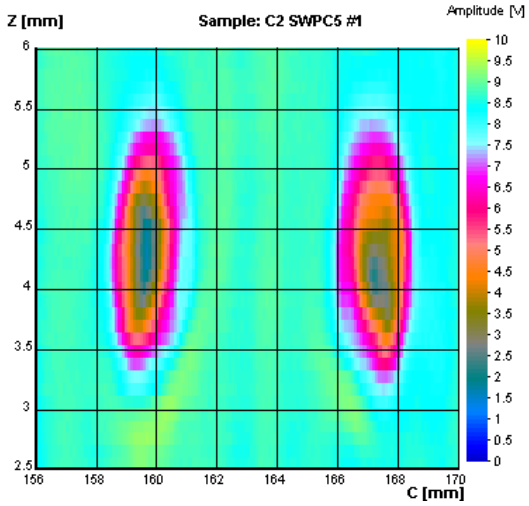

FIG. 24d. PC amplitude image of the blister C2-b.

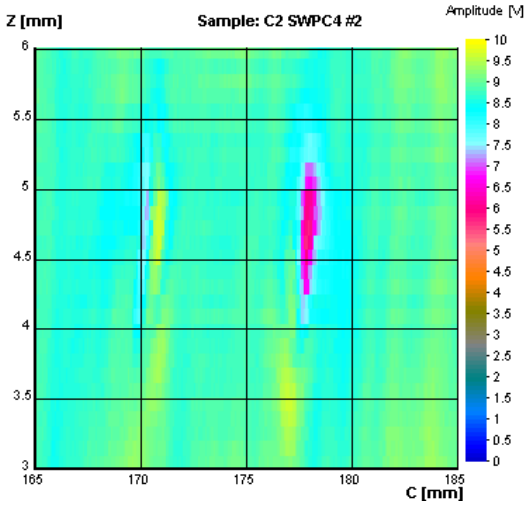

FIG. 24e. PC amplitude image of the blister C2-a.

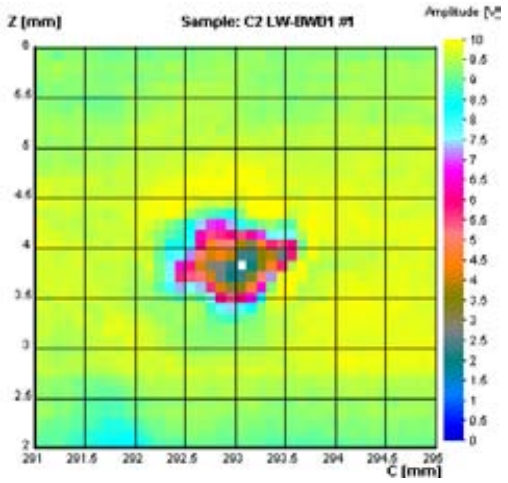

FIG. 25. Normal beam-amplitude drop (NA) image of the blister C2-b.

3.5. Intercomparison of results

Argentina, Canada and Romania-NNDT detected blisters by angle beam pulse-echo examination, although the reflected signal amplitude from majority of blisters were much lower than the ones from reference notches (CAN-CSA N285.4 [11]). Romania-NIRDTP could also detect blisters by orthogonal EC coil in send-receive mode, although the signal to noise ratio was much lower. Argentina could detect blisters by eddy current while performing examination from outside surface. Although, this technique will not be useful for in-situ applications, it holds a good potential during post irradiation examination of PT.

Romania-NNDT could detect four of the six blisters by normal beam backwall drop technique. The reason for this could be the use of much higher frequencies by Romania-NNDT (25 MHz and 50 MHz) compared to Argentina and Canada (10 MHz).

The blisters were best detected by Romania-NNDT using circumferential angle beam pitch-catch technique by monitoring the amplitude drop of the transmitted signal.

All the blisters showed varying degree of signal characteristics during various UT examinations. Blister C1-*a* was the most difficult to detect by any technique, while blister C2-*b* showed significant amplitude of the reflected signal.

3.6. Assessment and discussion of results

The results of examination on blister samples obtained by Argentina, Canada and Romania-NNDT indicates that the UT techniques applicable for flaw detection in PTs can be effective for blister detection as well. The same can also be said for ET using orthogonal coils. The UT results from all the laboratories indicate that although reflected signals were obtained from the majority of the blisters, the signals were much lower than the ones obtained from the reference notches made as per CAN-CSA-N285.4 [11]. In order to be more reliable, the reference defect standard for blister detection can be more stringent than the one used for flaw detection in PTs. There is also a need to improve signal-to-noise ratio by means of signal processing during UT and ET examination.

All the blisters showed varying degree of reflected signal amplitude during UT angle beam shear wave examination. However, it could not be differentiated whether the reflected signals were from the scratches in the tube from the region surrounding the blister, the geometrical feature of the blister or possible crack in the blister.

The angle beam pitch-catch technique is found to be most effective for blister detection. All the blisters, except one, were detected by this technique. The amplitude drop recorded by this technique is observed to be more than the reflected signal amplitude in angle beam pulse-echo technique. The backwall drop technique also gave good results on almost all the blisters. Although normal beam examination using 10 MHz was not found to be all that useful, the one carried out using 25 MHz and 50 MHz was effective. The normal beam backwall drop can very well compliment the circumferential angle beam pitch-catch technique. The angle beam shear wave pulse-echo was not found to be very reliable for blister detection, unless the blister is cracked.

The length and the width estimate could be made from amplitude C scan images. The angle beam pitch-catch technique performed better than others for this purpose. None of the techniques attempted during this CRP was able to estimate the depth of blister.

The blister samples circulated during this CRP were generated by Argentina. Their previous experience indicates that the blister generated by metallic cold fingers show cracking, even if its diameter is well within 1 mm. The blisters in PT samples A1, A2, C1 and C2 were generated by metallic cold finger. Hence, it is likely that some of the blisters examined during this exercise could be cracked. The higher reflected signal amplitude obtained from some of the blisters during angle beam pulse-echo examination could be attributed to that. The PT samples also have extensive scratches

surrounding the blister. These can contribute to lower amplitude reflected signals during angle beam examination. The presence of scratches or cracks in blisters can also contribute to the amplitude drop in angle beam pitch-catch and normal beam.

It can be concluded that a more stringent standard (in comparison to CAN-CSA N285.4 [11]) needs to be evolved for reliable detection of blister. New approaches like the amplitude drop in backwall examination and angle beam pitch-catch examination is more effective than the conventional angle beam pulse-echo examination. C scan imaging can give a good approximation on the length and width of the blister. New techniques (B scan imaging, Lamb waves, etc.) need to be developed for assessment of blister depth.

4. CONCLUSION AND RECOMMENDATIONS

4.1. Hydrogen determination

During this CRP, the participating laboratories employed various methods for hydrogen determination. These included the more established direct methods like HVE-MS and IGF and indirect method like DSC. These three methods need a small sample for analysis; hence they cannot be employed for in-situ hydrogen determination in PTs. The CRP also witnessed non-destructive examination methods based on ultrasonics (sound velocity measurement), eddy current (conductivity measurement) and resistivity measurement. While ultrasonic and eddy current tests were performed at room temperature under static condition, the resistivity-based measurements were performed under dynamic conditions. During resistivity test, the PT sample was taken through a heating and cooling cycle from room temperature to 400^{o}C. The TSS temperatures were determined and the hydrogen concentration is worked out from Arrhenius equation.

The following conclusions can be drawn from the analysis carried out by participating laboratories using the above methods on samples charged with varying levels of hydrogen:

(a) The direct methods like HVE-MS and IGF give an accurate estimate of hydrogen concentration in PTs. These methods performed consistently well for varying levels of hydrogen in the range of 5-100 ppm.

(b) HVE-MS and IGF results are less dependent on the equipment and the analysis procedure, provided appropriate reference standard and validated procedures are used.

(c) For DSC analysis, T_{SSP} and T_{SSD} are better indicators of hydrogen concentration than T_{mD}, T_{mP} and T_{onset}.

(d) Room temperature static tests using ultrasonics, based on sound velocity measurement, and eddy currents based on conductivity measurement does not show a significant change with varying levels of hydrogen in the range of 5-100 ppm. Hence at present, these techniques are not suitable for hydrogen determination in PTs.

(e) Resistivity based measurement has emerged as the promising NDE technique for determination of hydrogen in PTs.

The following recommendations are made for future collaborative work in this area:

(1) PT samples can be charged with Deuterium (D) instead of hydrogen. Under reactor conditions, the major hydrogen pick-up by PTs is in the form of deuterium and hence similar exercise with samples charged with varying levels of deuterium will be appropriate.

(2) The hydrogen (or deuterium) charging process should be validated to assess the expected hydrogen concentration before the samples are sent to participating laboratories by the originating laboratory. The amount of hydrogen charged should also be confirmed by metallography.

(3) The hydrogen charging temperature should be kept under the maximum temperature seen by PTs during their lifetime for generation of samples to be analyzed by indirect methods.

(4) For analysis using indirect methods like DSC, DTA and Resistivity the participating laboratories should use their own Arrhenius equation to assess hydrogen concentration corresponding to various temperatures. Such an equation can be generated using the primary or the secondary reference standards.

(5) The work carried out on resistivity-based measurements during this CRP needs to be extended for in-situ application.

(6) Dynamic measurements using ultrasonics and eddy current can be explored as a possible NDE method for in-situ hydrogen determination in PTs.

4.2. Blister characterization

During this CRP four PT samples with laboratory grown hydride blisters were prepared by Argentina. Two of these samples have two blisters each and the remaining two samples have one blister each. These were circulated to participating laboratories in round-robin manner. The laboratories employed ultrasonics and/or eddy current to detect and characterize blisters. The Argentinean experience on blister generation shows that the some of the blisters in PT samples used during this exercise could be cracked. Moreover, the PT surface in the region surrounding the blisters had several shallow and deep scratches.

The following conclusions can be drawn from the results of investigation carried out by participating laboratories on the blister samples:

(a) Ultrasonic testing performed better than eddy current for detection of blister while carrying out the test from inside surface of PTs.

(b) Angle beam pitch-catch based on amplitude drop detected all except one blister in all the samples.

(c) High frequency normal beam based on backwall drop using 25 MHz and 50 MHz performed better than 10 MHz.

(d) C scan imaging based on angle beam amplitude drop provides a good estimate of the length and the width of the blister.

(e) It remains inconclusive whether the signals obtained during ultrasonic testing were from the geometrical feature of the blister, the scratches surrounding the blister or the possible cracks in the blister.

(f) None of the NDE techniques used during this CRP could estimate the depth of the blister.

The following recommendations are made for future exercise of similar nature involving blister detection and characterization:

(1) Two sets of samples, one with un-cracked blister and other with the cracked ones can be generated.

(2) It should be verified by alternate means that the blister certified as un-cracked does not have crack(s).

(3) The PT sample used for blister generation should be free of any scratches on the outside surface.

(4) Reference defect standard needs to be evolved for setting-up the scanning sensitivity for blister detection during ultrasonics and eddy current tests.

REFERENCES

[1] INTERNATIONAL ATOMIC ENERGY AGENCY, Intercomparison of Techniques for Inspection and Diagnostics of Heavy Water Reactor Pressure Tubes, Flaw Detection and Characterization, IAEA-TECDOC-1499, Vienna, May (2006).

[2] MC MINN, A., DARBY, E.C., SCHOFIELD, J.S., "The terminal solid solubility of hydrogen in zirconium alloys", Zirconium in the Nuclear Industry: 12th International Symposium, G.P. Sabol and G.D. Moan editors. ASTM publication STP 1354. pp. 173-193, (2000).

[3] KEARNS, J.J., Dissolution kinetics of hydride platelets in zircaloy-4, J. Nucl. Mater. 22 (1967), 292.

[4] SLATTERY, G.F., The terminal solid solubility of hydrogen in zirconium alloys between 30 and 400°C, J. of the Institute of Metals, 95, (1967), 43.

[5] JOVANOVIC, M., STERN, A., KNEIS, H., WEATHERLY, G.C., LEGERS, M., Thermal diffusion of hydrogen and hydride precipitationin Zr-Nb pressure tube alloys, Can. Met. quarterly, 27, No. 4, (1988), 323.

[6] PAN, Z.I., RITCHIE, I.G., PULS, M.P., The terminal solid solubility of hydrogen and deuterium in Zr-2.5Nb alloys, J. Nucl. Mater. 228, (1996), 227.

[7] GOMEZ, M.P., DOMIZZI, G., PUMAREGA, M.I., RUZZANTE, J.E., Characterization of hydrogen content in Zry-4 using ultrasonic techniques, J. of. Nuclear Materials, Vol 353/3 (2006) pp 167-176.

[8] SAWATZKY, A., Hydriding Zircaloy-2 by Electrolyisis, AECL report No. 1046. Chalk River, Ontario (1960).

[9] CRANK, J., Mathematics of Diffusion, Oxford University Press, Oxford (1956).

[10] SKINNER, B.C., DUTTON, R.,Hydrogen Effects on Material Behavior, Edit. N.R. Moody and A.W. Thompson. The Minerals, Metals and Materials Societ, (1990), 73.

[11] CAN-CSA-N285.4-94, "Periodic inspection of CANDU nuclear power plant components".

CONTRIBUTORS TO DRAFTING AND REVIEW

Belinco, C.G.	Comisión Nacional de Energía Atómica (CNEA-CAC), Argentina
Chaplin, K.	AECL Chalk River Laboratories, Canada
Cheong, Y.-M.	Korea Atomic Energy Research Institute (KAERI), Republic of Korea
Choi, J.-H.	International Atomic Energy Agency
Cleveland, J.	International Atomic Energy Agency
Craig, S.	AECL Chalk River Laboratories, Canada
Domizzi, G.	Comisión Nacional de Energía Atómica (CNEA-CAC), Argentina
Grimberg, R.	National Institute of Research & Development for Technical Physics, Romania
Hébert, H.	AECL Chalk River Laboratories, Canada
Joulin, T.	AECL Chalk River Laboratories, Canada
Kulkarni, P.	Bhabha Atomic Research Centre, India
Mayo, W.	AECL Chalk River Laboratories, Canada
Nanekar, P.	Bhabha Atomic Research Centre, India
Ramadasan, P.	Bhabha Atomic Research Centre, India
Ruch, M.	Comisión Nacional de Energía Atómica (CNEA-CAC), Argentina
Sahoo, K.	Bhabha Atomic Research Centre, India
Shah, B.K.	Bhabha Atomic Research Centre, India
Soare, M.	S.C. Nuclear NDT Research & Services S.R.L. (NNDT), Romania
Zahn, N.	AECL Chalk River Laboratories, Canada